nature portfolio

Peer Review File

High-strength and high-modulus silicon monoxide for high-energy-density and fast-charging lithium-ion batteries

Corresponding Author: Professor Soojin Park

Parts of this Peer Review File have been redacted as indicated to remove third-party material.

This file contains all reviewer reports in order by version, followed by all author rebuttals in order by version.

Version 0:

Reviewer comments:

Reviewer #1

(Remarks to the Author)
The manuscript claims a LiF–SiO anode architecture that achieves simultaneously high modulus and high strength via domain-size control (Hall–Petch / inverse Hall–Petch) and a composite rule-of-mixtures rationale, reporting 108 GPa Young's modulus and markedly reduced residual stress/expansion, with improved transport from an a-LiF/F-doped carbon sheath.
However, there are quite a few concerning issues in the manuscript listed as follows. I do not think this manuscript is scientifically rigorous. The authors tried to tell an attractive story but the critical data reported in the manuscript lacks of sufficient evidence back which makes the manuscript unacceptable.
1. There is no experiment data for the stress-strain curve for the mechanical characterization of the newly fabricated anode materials. This is the first time in my career that I did not find any solid evidence support for a claimed parameter. And this parameter is the core selling point of this work. Without a rigorous stress-strain curve, one can never tell what the Young's modulus or yield stress is. Hall–Petch effect is only a theoretical guidance for the fabrication while it cannot guarantee nor the authors can infer the modulus or yield stress based on the theory alone.
2. The author also claimed better fatigue properties for the material and again, I did not find any mechanical cyclic loading for the material.
3. The lithiation of Si material is highly anisotropic so the authors also need to provide the mechanical characterization data for the anisotropicity.
4. You posit ~32 nm c-LiF domains as near the transition where classic to inverse Hall–Petch flips, maximizing strengthening. Please show a controlled size series (e.g., ~10, 20, 32, 50 nm c-LiF) and plot measured hardness/strength vs. $d^{-1/2}$ to verify the claimed optimum experimentally. Current support relies on literature rationale; without a size-dependent mechanical data set, the conclusion remains speculative.
5. The reduction to 7.0% expansion is central. Please detail the method (ex-situ caliper, cross-sectional SEM thickness, dilatometry, or in-operando stack-stress/dilatometry), sampling (n), and uncertainty. For high-loading Si anodes, in-operando dilatometry or stack-force traces would strongly support the claim.
6. The manuscript quotes 1.2×10^{-2} S cm^{-1} for a-LiF (very high for LiF-based phases). Please clarify measurement method (EIS on symmetric pellets? temperature? blocking electrodes?), microstructure (porosity, percolation with carbon), and rule out artifact paths (e.g., residual electrolyte). If this value is literature-based, cite and reconcile with known LiF conductivities.
7. The sheath is "tens to ~100 nm" yet is claimed to avoid kinetic penalties. Please quantify thickness distributions and relate them to the observed R_ct via modeling or controlled-thickness experiments to close the loop between mechanics (coverage) and kinetics (impedance).
8. What criterion defines the "residual stress" Raman peak selection, and how sensitive are stresses to peak-fit choices and local texture?

Reviewer #2

(Remarks to the Author)
This manuscript presents a synthetic strategy that creates crystalline lithium fluoride (c-LiF) domains in micrometer-scale SiO particles and forms a conductive outer sheath. The precise control of c-LiF domain size through the Hall-Petch

relationship and the rule of mixtures effectively improves both yield strength and Young's modulus of Si-based materials. The study systematically addresses mechanical failures in Si-based anodes through theoretical design principles and detailed structural characterization, thereby enabling fast-charging and energy-dense operation. Overall, this work could be suitable for Nature Communications, provided the points below are addressed.
1. While the authors provide a comprehensive discussion of various degradation mechanisms, including elastic/plastic deformation and fatigue, it would be helpful to expand the explanation of fatigue phenomena, as this concept may be less familiar to some readers in the lithium-ion battery community.
2. The manuscript would benefit from a quantitative comparison of volume expansion behavior between bare SiO and LiF-SiO particles after lithiation. Such measurements (for example, by comparing particle sizes in SEM images of fully lithiated materials) would provide additional evidence for the claimed mechanical improvements.
3. While Fig. 4f presents the influence of the a-LiF/F-doped carbon layer on SEI formation in the LiF-SiO electrode, further characterization using XPS depth-profiling would strengthen the proposed mechanism and enhance understanding of the compositional changes at the interface after cycling. The composition and structure of the interphase layer significantly influence the fast-charging performance of Si-based anodes (ref, Nature Communications, 2025, 16, 7956). A related discussion would help strengthen the understanding of the as-fabricated Si-based anode materials.
4. For the Young's modulus measurements reported in Fig. 2c, please specify the number of samples tested and whether the reported values represent average results with appropriate statistical analysis.
5. The 3D mapping data in Fig. 3c requires scale specification in the data boxes to enable better interpretation of the LiF spatial distribution observed in the TOF-SIMS analysis.

Reviewer #3

(Remarks to the Author)
The authors proposed a method for stabilizing the electrochemical activity of silicon-based electrodes - a problem which has been a subject of intense investigations over the past decade. The authors demonstrated a functional full cell even in a pouch cell format.
Despite interesting results, there is a number of experimental issues to be addressed:
1. The article claims the formation of LiF-SiO as a general principle, however, it's formation can only be achieved if the starting material originates from LG Energy Solutions, which is not a common chemical vendor. Therefore, this raises a question about reproducibility of the presented work as the starting materials are not obvious and were not fully characterized. Thus, while this approach is industrially interesting and relevant, I am not sure if this is of a broad interest of a scientific community.
2. The experimental part lack details: a) preparation - define ultrasonication, amount of toluene added to the mixture. b) Electrode preparation: why 10 % of the binder has been used? This should be justified, especially considering claimed stability. Was the electrode prepared through a dry processing or water-based (details are missing)? c) how many cells were evaluated? the presented data reflects a measurement of a single cell or average? d) Why FEC has been used in the electrolyte? Can the authors provide a comparison of electrolytes with and without FEC? e) The selected voltage window should be justified/explained. Generally, Si-based anodes are not cycled to 5 mV due to the formation of crystalline phase of lithiated silicon, which is believed to be detrimental for long-term cyclability of Si.
3. Figure 3. XRD peaks should be properly identified. In addtiion, a picture representing LiF2- is not clear - what is suppose to show?

Reviewer #4

(Remarks to the Author)
I co-reviewed this manuscript with one of the reviewers who provided the listed reports. This is part of the Nature Communications initiative to facilitate training in peer review and to provide appropriate recognition for Early Career Researchers who co-review manuscripts.

Version 1:

Reviewer comments:

Reviewer #1

(Remarks to the Author)
The authors have successfully addressed the questions and now the manuscript is ready for publication.

Reviewer #2

(Remarks to the Author)
The authors have well addressed all my concerns/questions. The current version of the manuscript with high quality is recommended for acceptance.

Reviewer #3

(Remarks to the Author)
I think the authors addressed the comments.

Reviewer #4

(Remarks to the Author)
I co-reviewed this manuscript with one of the reviewers who provided the listed reports. This is part of the Nature Communications initiative to facilitate training in peer review and to provide appropriate recognition for Early Career Researchers who co-review manuscripts.

Response to the Reviewers' Comments

(Nature Communications - Manuscript ID: NCOMMS-25-65475)

Title: "High-strength, high-modulus silicon monoxide for high-energy-density and fast-charging lithium-ion batteries"

* All of the modifications in the revised version are highlighted in yellow color.

Reviewers' comments as follows;

Reviewer# 1

***Comments**: The manuscript claims a LiF–SiO anode architecture that achieves simultaneously high modulus and high strength via domain-size control (Hall–Petch / inverse Hall–Petch) and a composite rule-of-mixtures rationale, reporting 108 GPa Young's modulus and markedly reduced residual stress/expansion, with improved transport from an a-LiF/F-doped carbon sheath.*

However, there are quite a few concerning issues in the manuscript listed as follows. I do not think this manuscript is scientifically rigorous. The authors tried to tell an attractive story but the critical data reported in the manuscript lacks of sufficient evidence back which makes the manuscript unacceptable.

Response: We sincerely appreciate the reviewer's detailed feedback and the opportunity to strengthen our manuscript. We have addressed each concern by substantially expanding our experimental validation, including comprehensive mechanical characterization, systematic structure-property studies, and additional supporting data.

Our work introduces a critical but overlooked aspect of Si-based anode design. While conventional strategies focus exclusively on enhancing Young's modulus to resist elastic deformation, we demonstrate that yield strength—which governs resistance to plastic deformation and cyclic fatigue—is equally essential for long-term stability. By strategically incorporating c-LiF domains with optimized size distribution into the SiO_2 matrix, we simultaneously achieve high Young's modulus and elevated strength. This dual mechanical reinforcement, complemented by ionically conductive a-LiF/electronically conductive F-doped carbon sheaths, enables superior electrochemical performance under demanding cycling conditions.

To address the reviewer's concerns, we have added comprehensive mechano-electrochemical characterization:

- Particle strength measurements comparing bare SiO, Li-SiO, and LiF-SiO (newly updated Fig. **2**c and Supplementary Fig. 7).

- Strength vs. $d^{-1/2}$ analysis across c-LiF domain sizes, and direct correlation between mechanical reinforcement and cycling stability, experimentally verifying Hall–Petch transition and ~32 nm optimum (Supplementary Fig. 11).

- In situ measurement of thickness evolution of bare SiO, Li-SiO, and LiF-SiO electrodes during the initial 3 cycles, quantifying electrode-level volumetric fluctuation (Supplementary Fig. 23).

- Cross-sectional SEM imaging of individual particles before and after lithiation, prepared via cross section polisher (CP), to directly visualize and quantify particle-level changes in mean Feret diameter (Supplementary Fig. 22).

- Systematic evaluation of sheath thickness effects on mechanical and electrochemical properties with comprehensive characterization (TEM, EIS, electrochemical performance) (Supplementary Fig. 14).

- XPS depth profiling analysis to provide in-depth characterization of the outer layer, including a-LiF/F-doped carbon sheath and SEI layer (Supplementary Fig. 18).

- Enhanced experimental/technical/statistical rigor.

These additions provide robust experimental validation of our proposed mechanisms and design principles. We believe the revised manuscript now presents a scientifically rigorous and well-supported narrative that meets the high standards of Nature Communications. We are grateful for the reviewer's critical feedback, which has substantially improved our work.

Comment 1-1: *There is no experiment data for the stress-strain curve for the mechanical characterization of the newly fabricated anode materials. This is the first time in my career that I did not find any solid evidence support for a claimed parameter. And this parameter is the core selling point of this work. Without a rigorous stress-strain curve, one can never tell what the Young's modulus or yield stress is. Hall–Petch effect is only a theoretical guidance for the fabrication while it cannot guarantee nor the authors can infer the modulus or yield stress based on the theory alone.*

Response 1-1: We sincerely appreciate the reviewer's insightful comment, which strengthens the rigor of our work. In response, we have added particle-level strength measurements.

Combined with the Young's modulus results presented in the initial submission, these data now provide complete experimental validation of our mechanical reinforcement strategy.

We performed single-particle compression tests using a micro compression testing machine (Shimadzu, MCT-510) to directly measure particle strength (Supplementary Fig. 7). The stress-displacement curves reveal particle strength: bare SiO (698.7 MPa), Li-SiO (895.7 MPa), and LiF-SiO (5532.1 MPa). The nearly 8-fold strength enhancement in LiF-SiO provides direct experimental evidence validating our mechanical reinforcement strategy. Complementing the Young's modulus results (bare SiO: 34.0 GPa, Li-SiO: 51.8 GPa, LiF-SiO: 108.1 GPa), these measurements now provide comprehensive mechanical characterization demonstrating that c-LiF incorporation substantially enhances both plastic and elastic deformation resistance (Fig. **2**c).

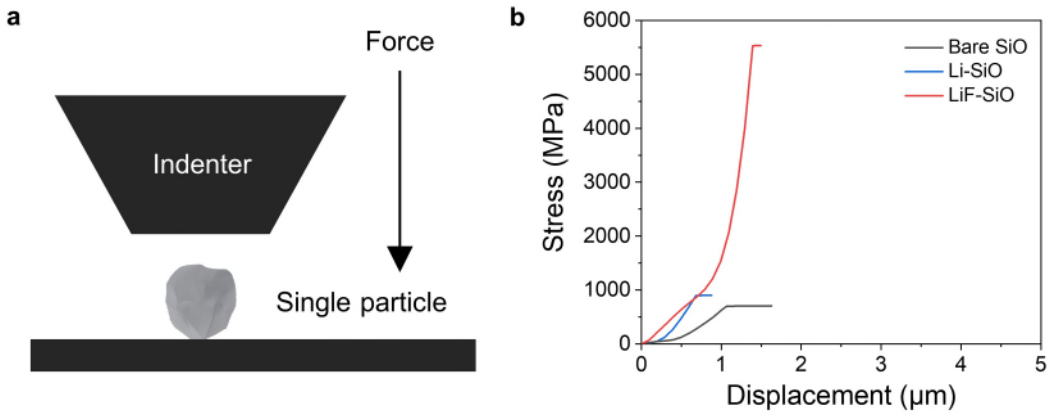

Supplementary Fig. 7 | Particle strength measurement. a Schematic illustration of the microcompression test performed on a single particle. **b** Stress-displacement curves of bare SiO, Li-SiO, and LiF-SiO particles to determine strength.

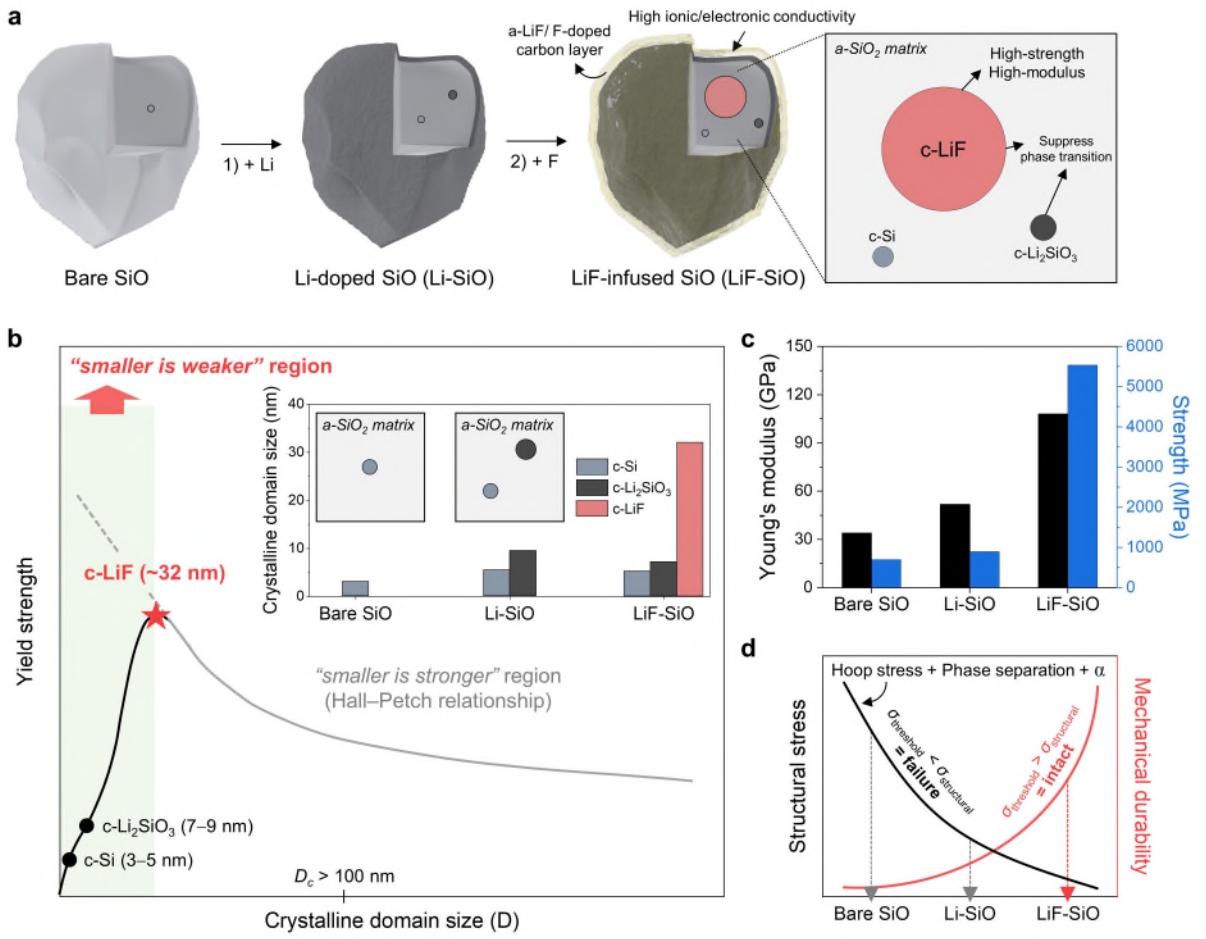

Fig. 2 | Infiltrative coating of LiF for high-strength, high-modulus SiO. a Schematic illustration for the synthesis of LiF-SiO through sequential Li doping and F infusion processes. **b** Semiquantitative illustration of yield strength versus crystalline domain size; the gray curve represents the traditional Hall–Petch relationship ("smaller is stronger"), while the black curve depicts the inverse Hall–Petch behavior ("smaller is weaker") observed in nanocrystalline materials below a critical size threshold (Inset: comparison of crystalline domain sizes within bare SiO, Li-SiO, and LiF-SiO). **c** Experimentally measured Young's modulus (black) and strength (blue) of bare SiO, Li-SiO, and LiF-SiO particles. **d** Schematic graph showing the relationship between structural stress and mechanical durability of bare SiO, Li-SiO, and LiF-SiO under repeated (de)lithiation process.

Importantly, post-mortem SEM analysis (Fig. **5**d) confirms that this mechanical reinforcement enables structural stability under repeated cycling stress from volumetric changes. LiF-SiO particles maintain integrity after extended cycling, while bare SiO exhibits extensive cracking and pulverization. Our electrochemical cycling data, combined with these mechanical measurements, provide a compelling demonstration that particle-level mechanical enhancement is the key enabler of superior performance.

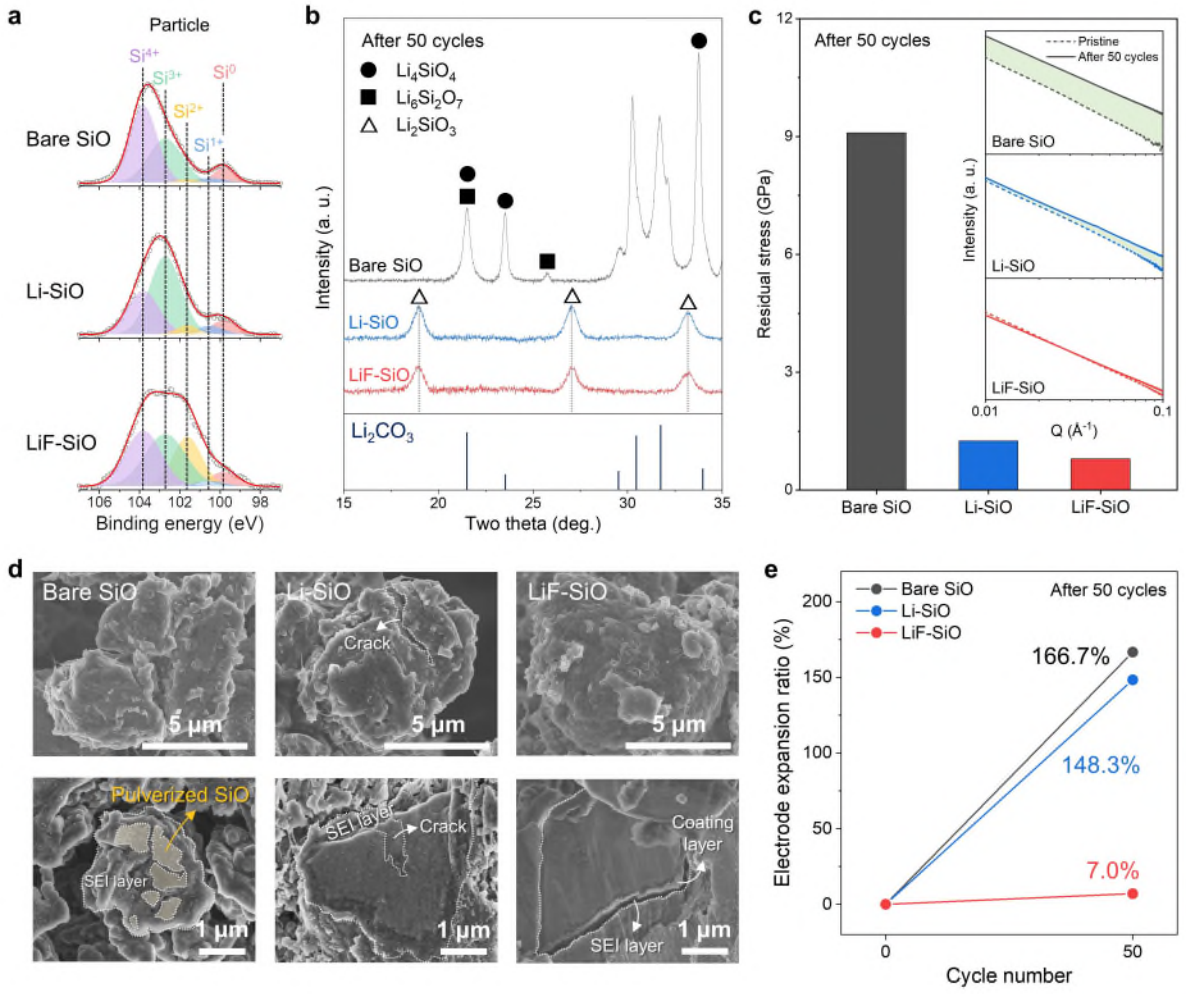

Fig. 5 | Chemo-mechanical characteristics of LiF-SiO after repeated (de)lithiation process. a Si 2p XPS spectra of bare SiO, Li-SiO, and LiF-SiO particles. **b** XRD patterns and **c** residual stress of bare SiO, Li-SiO, and LiF-SiO electrodes after 50 cycles at 2C (Inset: SAXS intensity profiles of the three electrodes). **d** Magnified SEM images (top) and cross-sectional views prepared by ion milling (bottom) of bare SiO, Li-SiO, and LiF-SiO electrodes after 50 cycles at 2C. **e** Electrode expansion ratio of bare SiO, Li-SiO, and LiF-SiO after 50 cycles at 2C.

We acknowledge that the Hall–Petch effect served as theoretical guidance for our design. However, we now provide rigorous experimental mechanical characterization rather than relying on theory alone. Our expanded discussion and corresponding experimental details have been added to the revised manuscript and Supplementary Information. Please see Fig. **2**c and the Methods section in the revised manuscript, and Supplementary Fig. 7 in the Supplementary Information.

[7 page] *"Our design principles, combined with the Hall–Petch effect and the rule of mixtures, yield improved mechanical properties. Experimentally, LiF-SiO achieves a Young's modulus of 108.1 GPa, markedly exceeding bare SiO (34.0 GPa) and Li-SiO (51.8 GPa) (Fig.* **2***c). Moreover, c-LiF size optimization substantially reinforces particle strength of LiF-SiO (5532.1 MPa), which significantly surpasses bare SiO (698.7 MPa) and Li-SiO (895.7 MPa) (Supplementary Fig. 7). This strength–modulus synergy addresses two distinct failure modes arising from the hoop stress."*

[22 page] *"Reported values represent the mean of five independent measurements (n = 5) per sample. A micro compression testing machine (Shimadzu, MCT-510) was used to measure the single-particle strength. SAXS measurements were conducted at the 4C SAXS II beamline (BL) of the PLS-II facility with 3 GeV power, Pohang Accelerator Laboratory …"*

Comment 1-2: *The author also claimed better fatigue properties for the material and again, I did not find any mechanical cyclic loading for the material.*

Response 1-2: We appreciate the reviewer's powerful comments that help strengthen our work. During electrochemical cycling, the repeated volumetric expansion and contraction of Si generate cyclic stresses within the particle or composite structure. The magnitude of these stresses scales with Si particle (or Si domain in composite materials) size; below ~150 nm, individual stress levels remain insufficient to cause immediate fracture (*ACS Nano* **2012**, 6, 1522–1531). However, when such sub-yield stresses are repeatedly applied over many cycles, the cumulative mechanical loading progressively weakens the material through a process called fatigue. Fatigue causes crack initiation and propagation not through a single catastrophic event, but through accumulated damage from each cycle (Fig. R1).

[Figure Redacted]

Fig. R1. Mechanical characterizations of Li metal. (A-C) In-situ tensile testing and (D-F) fatigue testing of Li metal with a maximum stress of 0.65 times its tensile strength. The scale bar is 300 μm (*Science* **2025**, 388, 311).

Since the threshold for fatigue failure increases with yield strength, elevating strength through c-LiF size engineering directly enhances fatigue resistance by expanding the safe operating window for cyclic loading. Therefore, our electrochemical cycling data, combined with this microstructural evidence discussed in **Response 1-1**, provide a compelling demonstration of enhanced fatigue resistance resulting from strength improvement. In response, we have added a corresponding discussion in the revised manuscript. Please see the revised manuscript.

[7 page] *"This strength–modulus synergy addresses two distinct failure modes arising from the hoop stress. First, high strength mitigates plastic deformation and potential fatigue. Notably, fatigue is defined as the process where repeated (de)lithiation cycles impose continuous mechanical loading (despite individual stress levels remaining below the yield strength) that causes material degradation and cracking, which is particularly critical in Si-based anodes. Since the threshold for fatigue failure increases with yield strength, elevating strength directly enhances fatigue resistance. Second, increased modulus minimizes mechanical strain under applied stress, thereby regulating volumetric changes and microstructural collapse."*

Comment 1-3: *The lithiation of Si material is highly anisotropic so the authors also need to provide the mechanical characterization data for the anisotropicity.*

Response 1-3: We appreciate the reviewer's insightful comment regarding the anisotropic lithiation nature of Si materials. We would like to clarify that while crystalline Si indeed exhibits significant anisotropic lithiation behavior, the mechanical implications of this anisotropy in our SiO system ultimately converge to the composite-level strength and modulus enhancement that forms the central focus of our study.

Our SiO composite material consists of nanoscale Si domains (3–5 nm) dispersed within an amorphous SiO_2 matrix, as confirmed by XRD and TEM analyses. While anisotropic stress concentration does occur preferentially along (110) planes during cycling—a characteristic feature of crystalline Si—the consequences of this anisotropy manifest differently at this ultrasmall domain size (below the critical fracture threshold of ~150 nm). In particles above 150 nm, anisotropic stress leads to directional crack propagation and catastrophic failure. However, in our 3–5 nm Si domains, the anisotropic stress field cannot generate sufficient strain energy for crack nucleation. Instead, the mechanical response is governed by elastic/plastic deformation and fatigue, where the composite's ability to accommodate anisotropic strain without permanent damage becomes paramount (Fig. R2).

[Figure Redacted]

Fig. R2. Scanning transmission electron microscopy (STEM) images of silicon particles from an uncycled electrode (upper left panel) and after different number of full (de-)lithiation cycles (*J. Electrochem. Soc.* **2018**, 165**,** A1503).

Critically, the localized stress generated at Si domains during lithiation must be endured by the surrounding SiO_2 matrix to prevent composite-level mechanical failure. While the SiO_2 matrix distributes and accommodates stress to suppress overall volumetric expansion (Fig. R3), both the stress-generating Si domains and the stress-bearing matrix experience structural transformation during cycling that compromises their load-bearing capacity if left unaddressed. Given that anisotropic lithiation in the Si domain and its associated inhomogeneous stress represent intrinsic and unavoidable phenomena, our LiF incorporation and domain size engineering address this challenge through bulk-level reinforcement. Based on Hall–Petch relationship and rule of mixtures for composites, we elevate the composite's overall strength and modulus, thereby enabling the structure to withstand the repetitive stress cycles imposed by Si (de)lithiation.

[Figure Redacted]

Fig. R3. Amorphous structures of Li_xSiO_y systems with x = 2 and y = 0, 0.1, 0.2, 0.3, 0.4, and 0.5 (left). Evolution of relative volume and density with increasing Li concentration (right) (*J. Power Sources* **2016**, 307, 657–664).

Consequently, the critical question shifts from managing anisotropic fracture (which does not occur at this size scale) to enhancing the composite's resistance against elastic/plastic deformation and fatigue. The anisotropic lithiation characteristics, rather than being a separate concern, directly underscore why composite-level mechanical enhancement is essential: the preferential stress concentration along specific crystallographic planes creates localized plastic

strain that can only be mitigated through elevated mechanical strength of the composite material. Our LiF incorporation strategy directly addresses this fundamental challenge throughout the cycling process. We have added corresponding text in the manuscript to acknowledge this anisotropic characteristic. Please see the revised manuscript.

[3 page] *"… emerge as promising candidates, offering a theoretical capacity tenfold higher than graphite counterparts and a low redox potential, both beneficial for high-energy-density applications[4]. However, the intrinsic alloying mechanism of Si upon Li storage, combined with anisotropic lithiation behavior, induces large and inhomogeneous volumetric fluctuations during the cycle, generating significant internal stresses—particularly hoop stress—within the particles[5]. This fundamental chemo-mechanical challenge provokes particle fracture, pulverization, and electrode delamination, accompanied by persistent reformation of solid-electrolyte-interphase (SEI) layers[6]."*

[7 page] *"Given that anisotropic lithiation in the Si domain and its associated inhomogeneous stress evolution represent intrinsic and unavoidable phenomena, integrating tailored-sized LiF domains into SiO underpins the structural robustness of LiF-SiO via the rule of mixtures for composites."*

Comment 1-4: *You posit ~32 nm c-LiF domains as near the transition where classic to inverse Hall–Petch flips, maximizing strengthening. Please show a controlled size series (e.g., ~10, 20, 32, 50 nm c-LiF) and plot measured hardness/strength vs. $d^{-1/2}$ to verify the claimed optimum experimentally. Current support relies on literature rationale; without a size-dependent mechanical data set, the conclusion remains speculative.*

Response 1-4: We appreciate this important comment regarding c-LiF domain size optimization. In response, in addition to literature-based guidance, we have carefully added experimental validation for the size-dependent strength and its correlation with cycling stability. To isolate this variable from competing effects (including total fluorine amount and outer sheath thickness), we conducted controlled synthesis using the same fluorinated carbon content while varying the heat treatment temperature (500, 600, 700, and 800 °C) (Supplementary Fig. 11). This approach solely modulates c-LiF domain size through temperature-dependent F infusion kinetics and crystallization, while preserving all other structural properties.

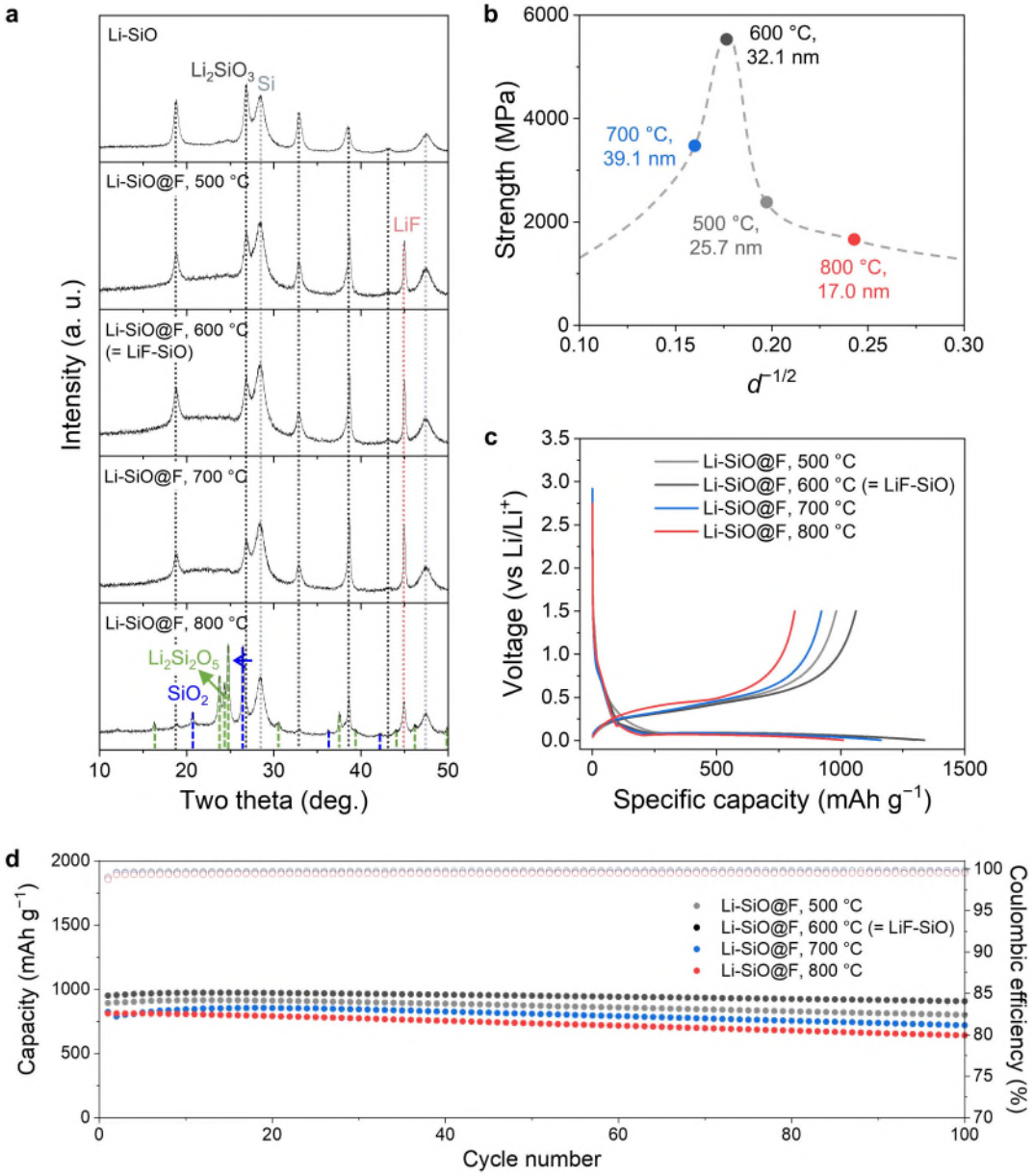

Supplementary Fig. 11 | Effects of crystalline LiF domain size on mechanical and electrochemical properties. a XRD patterns of Li-SiO(@F) before and after F infusion at varying heat treatment temperatures, **b** corresponding strength versus $d^{-1/2}$ curve, **c** galvanostatic charge/discharge profiles, and **d** cycle stability at 0.5 C.

XRD analysis confirmed distinct c-LiF domain sizes depending on heat treatment temperature: 25.7 nm (500 °C), 32.1 nm (600 °C), 39.1 nm (700 °C), and 17.0 nm (800 °C) (Supplementary Fig. 11). Notably, the 800 °C sample exhibited a smaller domain size due to severe disproportionation reactions at elevated temperature, which induced structural degradation and inhibited proper crystal growth.

Corresponding particle strength measurements plotted against $d^{-1/2}$ demonstrate the (inverse) Hall–Petch relationship with clear optimization around ~32 nm. This domain size represents the transition point where classic Hall–Petch strengthening shifts to inverse Hall–Petch behavior, thereby maximizing mechanical reinforcement. Importantly, electrochemical characterization corroborates these mechanical findings. The initial reversible capacity decreases with increasing temperature, attributable to irreversible consumption of pre-inserted Li during extensive LiF formation at higher temperatures and progressive structural degradation. Electrochemical cycling stability further supports these mechanical findings: the 600 °C sample (~32 nm c-LiF) exhibits superior long-term performance compared to other domain sizes, directly validating that mechanical optimization translates to enhanced cycling stability. The maximized strength effectively suppresses particle-level mechanical degradation, preventing the accumulation of structural damage that would otherwise limit cycle life.

This comprehensive experimental evidence—spanning structural characterization, mechanical measurements, and electrochemical validation—provides rigorous verification of the ~32 nm optimum. In this regard, we have added an expanded discussion in the revised manuscript and Supplementary Information. Please see the revised manuscript and Supplementary Fig. 11.

[9 page] *"… Critically, controlled synthesis conditions further enabled systematic modulation of c-LiF domain size from 17.0 to 39.1 nm, with ~32 nm domains approaching the critical size regime where classic-to-inverse Hall–Petch transition maximizes mechanical reinforcement (Supplementary Fig. 11). Note that annealing above 800 °C for F impregnation induced severe disproportionation reactions and structural disorder, manifested by the formation of crystalline SiO_2 and $Li_2Si_2O_5$ phases (20.7°, 24.7–24.8°) alongside paradoxically smaller c-LiF domains*[39,40]*. …"*

Comment 1-5: *The reduction to 7.0% expansion is central. Please detail the method (ex-situ caliper, cross-sectional SEM thickness, dilatometry, or in-operando stack-stress/dilatometry), sampling (n), and uncertainty. For high-loading Si anodes, in-operando dilatometry or stack-force traces would strongly support the claim.*

Response 1-5: We appreciate the reviewer's powerful comment regarding electrode-level volumetric stability. The 7.0% expansion value was obtained through cross-sectional SEM thickness measurements after 50 cycles at 2C, as shown in Supplementary Fig. 24. For accurate comparison, each material (bare SiO, Li-SiO, and LiF-SiO) was coated onto large-area electrode sheets with identical areal mass loading on the same day. From each sheet, two electrodes were punched—one analyzed immediately (pristine) and one after 50 cycles—to eliminate batch-to-batch variations. Representative images were selected by identifying regions exhibiting average thickness changes across multiple measurement locations to ensure reproducibility.

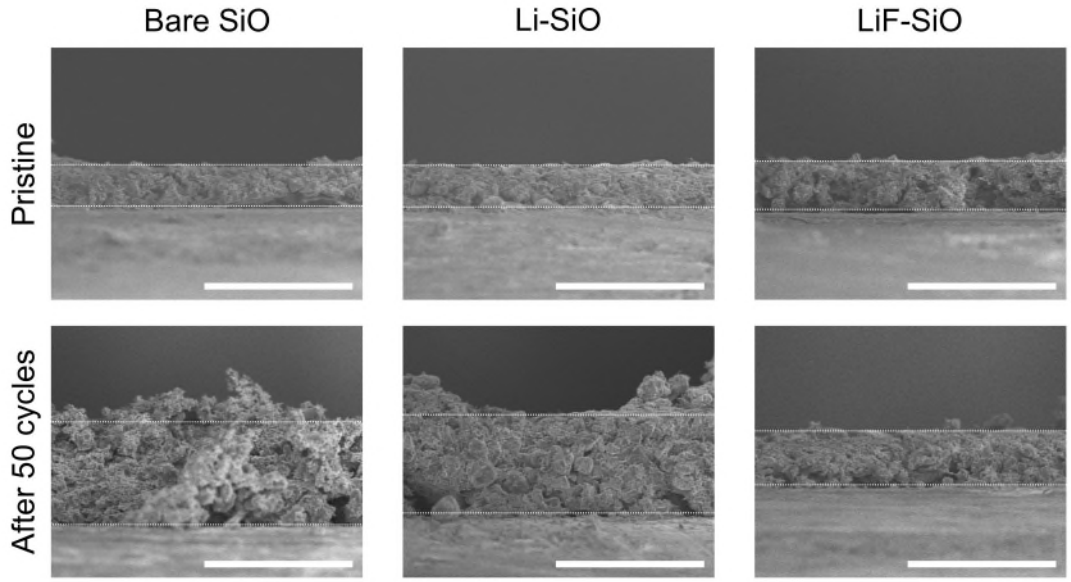

Supplementary Fig. 24 | Cross-sectional SEM analysis. Cross-sectional SEM images of bare SiO, Li-SiO, and LiF-SiO electrodes: Pristine and after 50 cycles (Scale bar: 50 μm).

Following the reviewer's valuable suggestion, we further conducted in situ thickness measurements of bare SiO, Li-SiO, and LiF-SiO electrodes during the initial 3 cycles to confirm electrode volume expansion/contraction behavior. As shown in Supplementary Fig. 23, bare SiO and Li-SiO electrodes exhibit severe volumetric expansion of 86.0% and 73.3% during the first lithiation, respectively. After one formation cycle, their irreversible thickness increases converge to 63.2% and 49.3%, respectively, indicating persistent structural instability. In contrast, the LiF-SiO electrode exhibits significantly suppressed initial lithiation expansion, with only 19.9% expansion, and an irreversible thickness increase of merely 3.6% after the same formation cycle.

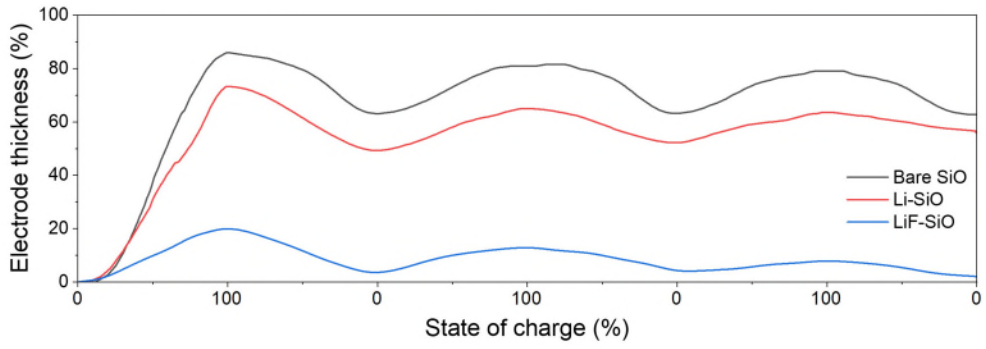

Supplementary Fig. 23 | Electrode swelling analysis. In situ thickness measurements of bare SiO, Li-SiO, and LiF-SiO electrodes during the initial 3 cycles.

Additionally, to directly correlate particle-level mechanical improvement with electrode-level volumetric stability, we performed cross-sectional analysis of individual particles within electrodes after the first lithiation. Cross section polisher (CP) coupled with SEM enabled precise visualization of particle dimensions embedded in the electrode matrix. All cross-sectioned particles displayed in each image were analyzed to quantify the mean Feret diameter using ImageJ software (at least 50 particles per sample to ensure statistical reliability). As shown in Supplementary Fig. 22, bare SiO particles exhibit severe dimensional changes from 4.24 μm to 6.94 μm (63.7%), and the corresponding electrode thickness increases by 72.3%. Similarly, Li-SiO particles show a 53.9% increase in diameter (3.95 μm → 6.08 μm) and electrode-level expansion of 64.9%. Remarkably, mechanically reinforced LiF-SiO particles exhibit only 18.9% increase in particle size (4.34 μm → 5.16 μm), with the electrode thickness increasing 22.4%.

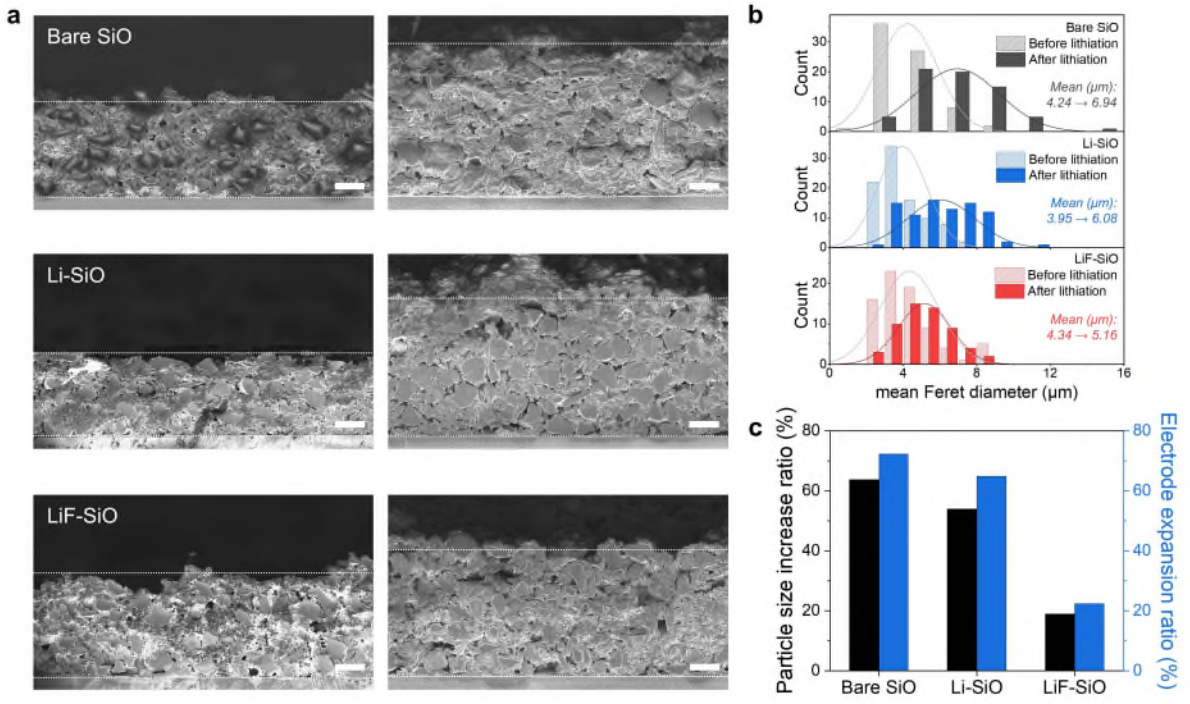

Supplementary Fig. 22 | CP–SEM analysis. a Cross-sectional SEM images of bare SiO, Li-SiO, and LiF-SiO particles within electrodes before (left) and after (right) the first lithiation, prepared using cross section polisher (CP). **b** Distribution of particle sizes (mean Feret diameter) before and after the first lithiation, and **c** Particle size increase and electrode expansion ratios in bare SiO, Li-SiO, and LiF-SiO electrodes after the first lithiation. Scale bars are 10 μm.

This substantial difference directly reflects how particle-level mechanical reinforcement governs electrode-level volumetric stability. Elevated strength and modulus suppress plastic deformation and permanent volume changes within individual particles, which collectively prevent the accumulation of irreversible expansion throughout the electrode. These observations agree excellently with the expansion ratios observed after 50 cycles. The LiF-SiO electrode maintains a compact structure with minimal SEI thickening, as shown in post-mortem particle SEM images (Fig. **5**d), whereas bare SiO and Li-SiO electrodes suffer from severe electrode expansion and microscopic degradation. The consistent volumetric behavior captured by in situ electrode thickness measurements and CP–SEM analysis corroborates that the incorporation of optimized LiF domains effectively mitigates electrode-level swelling throughout prolonged cycling, validating our proposed Type C architecture design strategy. In this regard, we have added an expanded discussion in the revised manuscript and Supplementary Information. Please see the revised manuscript and Supplementary Figs. 22 and 23.

[14 page] *"These particle-scale advancements translated to macroscopic electrode integrity. The optimized c-LiF incorporation in LiF-SiO not only suppressed phase separation but also imparted particle-level mechanical reinforcement, collectively reducing stress susceptibility and volumetric fluctuation. Cross-sectional polisher (CP) coupled with SEM revealed that LiF-SiO particles exhibited only 18.9% increase in particle size (mean Feret diameter) after the first lithiation, substantially lower than bare SiO (63.7%) and Li-SiO (53.9%) (Supplementary Fig. 22). In situ electrode thickness measurements demonstrated that this particle-level mechanical constraint directly manifested in electrode-level stability. During the first lithiation, LiF-SiO electrodes expanded only 19.9% compared to 86.0% (bare SiO) and 73.3% (Li-SiO), with irreversible expansion after the formation cycle reaching 3.6% versus 63.2% (bare SiO) and 49.3% (Li-SiO) (Supplementary Fig. 23). Expansion ratios after 50 cycles at 2C further quantified this sustained advantage; 166.7% (bare SiO), 148.3% (Li-SiO), and 7.0% (LiF-SiO) (Fig. **5**e and Supplementary Fig. 24). Similarly, EIS measurements confirmed that LiF-SiO electrode substantially reduced internal impedance, …"*

[21 page] *"… revealed the SEI thickness and the extent of particle cracking and pulverization after cycling. Cross section polisher (CP, IB-19520CCP, JEOL) coupled with SEM (GeminiSEM 560, ZEISS) was utilized to visualize particle-level and electrode-level changes after the first lithiation. All cross-sectioned particles displayed in each image were analyzed to quantify the mean Feret diameter using ImageJ software (at least 50 particles per sample to ensure statistical reliability). In situ measurement of electrode thickness evolution during the initial 3 cycles was conducted using an HS Swell Analysis Cell (Wellcos) with $Li(Ni_{0.80}Co_{0.10}Mn_{0.10})O_2$ (NCM811) cathode as the counter electrode at an N/P ratio of ~1.05 to attribute the measured thickness changes predominantly to the anode. The physical and chemical characterization of both the particle interior and its outermost region …"*

Comment 1-6: *The manuscript quotes 1.2×10^{-2} S cm^{-1} for a-LiF (very high for LiF-based phases). Please clarify measurement method (EIS on symmetric pellets? temperature? blocking electrodes?), microstructure (porosity, percolation with carbon), and rule out artifact paths (e.g., residual electrolyte). If this value is literature-based, cite and reconcile with known LiF conductivities.*

Response 1-6: We appreciate the reviewer's comment, which will strengthen our manuscript. This value is derived from density functional theory (DFT) calculations in Fig. R4 (*Acta Mater.* **2022**, 235, 118077), as direct experimental measurement of pure a-LiF is challenging—most literature reports conductivity of composite layers containing LiF rather than isolated a-LiF phases.

The reviewer correctly notes that crystalline LiF is well known to exhibit ionic conductivity of ~10^{-9}–10^{-13} S cm^{-1}. However, recent studies demonstrate that structural disorder and reduced crystallite size in LiF dramatically enhance its ionic conductivity (*Nat. Energy* **2025**, 10, 1132–1145; *Nature* **2025**, 646, 102–107). The DFT-predicted value aligns with this emerging understanding of disordered LiF systems.

Our electrochemical performance—excellent rate capability and stable fast-charging cycling —is consistent with ionically conductive a-LiF facilitating Li^+ transport. We have clarified in the revised manuscript that this value is computationally derived. Please see the revised manuscript.

[Figure Redacted]

Fig. R4. (a) Predicted ionic conductivity (σ_{Li}) in bulk c-LiF, a-LiF, and a-LiF(N). (b) Density of states (DOS) of c-LiF and a-LiF(N) with two different N contents (x = 14%, 25%). The vertical dashed line indicates the Fermi level position in a-LiF(N). Inset shows band-decomposed charge density isosurfaces (± 0.06 e/$Å^3$) for the localized states in the bandgap as indicated with a parenthesis (*Acta Mater.* **2022**, 235, 118077).

[6 page] *"The LiF-SiO architecture comprises c-Si, c-Li_2SiO_3, and c-LiF interspersed within an a-SiO_2 matrix, with substantial a-LiF integrated into the peripheral F-doped carbon layer. The a-LiF exhibits high ionic conductivity (1.2×10^{-2} S cm^{-1}, theoretically calculated value) and the F-doped carbon accelerates electron conduction, both of which facilitate charge transport at the particle surface (Supplementary Fig. 5)."*

Comment 1-7: *The sheath is "tens to ~100 nm" yet is claimed to avoid kinetic penalties. Please quantify thickness distributions and relate them to the observed R_ct via modeling or controlled-thickness experiments to close the loop between mechanics (coverage) and kinetics (impedance).*

Response 1-7: We thank the reviewer for suggesting the comments to improve our work. To isolate the effect of sheath thickness on electrochemical kinetics, we varied Li-SiO-to-fluorinated carbon ratios (4:1, 4:2, 4:3, 4:4) under otherwise identical synthesis conditions—where 4:2 represents the standard LiF-SiO composition—and evaluated the resulting structural and electrochemical characteristics (Supplementary Fig. 14).

As shown in the TEM images, increasing the fluorinated carbon content progressively thickens the a-LiF/F-doped carbon layer. The electrochemical evaluation across these thickness variations revealed competing effects. Higher fluorinated carbon ratios resulted in decreased initial Coulombic efficiency (ICE) due to the irreversible consumption of pre-inserted Li and a reduced specific capacity attributed to increased inactive mass. Additionally, the impedance analysis demonstrated an increased R_{SEI} resulting from the extended charge transport pathway through thicker coating layers. However, this transport resistance (R_{SEI}) is offset by significantly improved charge transfer kinetics (R_{ct}) at the sheath/inner particle interface. Complete interfacial coverage by ionically conductive a-LiF and electronically conductive F-doped carbon facilitates Li^+ insertion/extraction into the particle core, as evidenced by decreased R_{ct} values. Notably, at the highest ratios (4:3 and above), ICE values approached or fell below those of bare SiO, indicating that excessive R_{SEI} imposes kinetic penalties that outweigh the interfacial benefits.

The 4:2 ratio represents the optimal composition, providing mechanical robustness against volume changes while maintaining acceptable specific capacity and ICE. Critically, despite coating thicknesses reaching tens to ~100 nm, the balanced R_{SEI} and R_{ct} values prevent kinetic bottlenecks, enabling efficient charge transport.

This establishes a critical design principle: protective coatings for micrometer-scale Si-based materials must be thick enough (tens of nanometers) to withstand volume expansion, yet this thickness does not inherently impose kinetic limitations when interfacial properties are optimized. In response, we have substantially expanded our experimental validation in the revised manuscript. Please see the revised manuscript and Supplementary Fig. 14 in Supplementary Information.

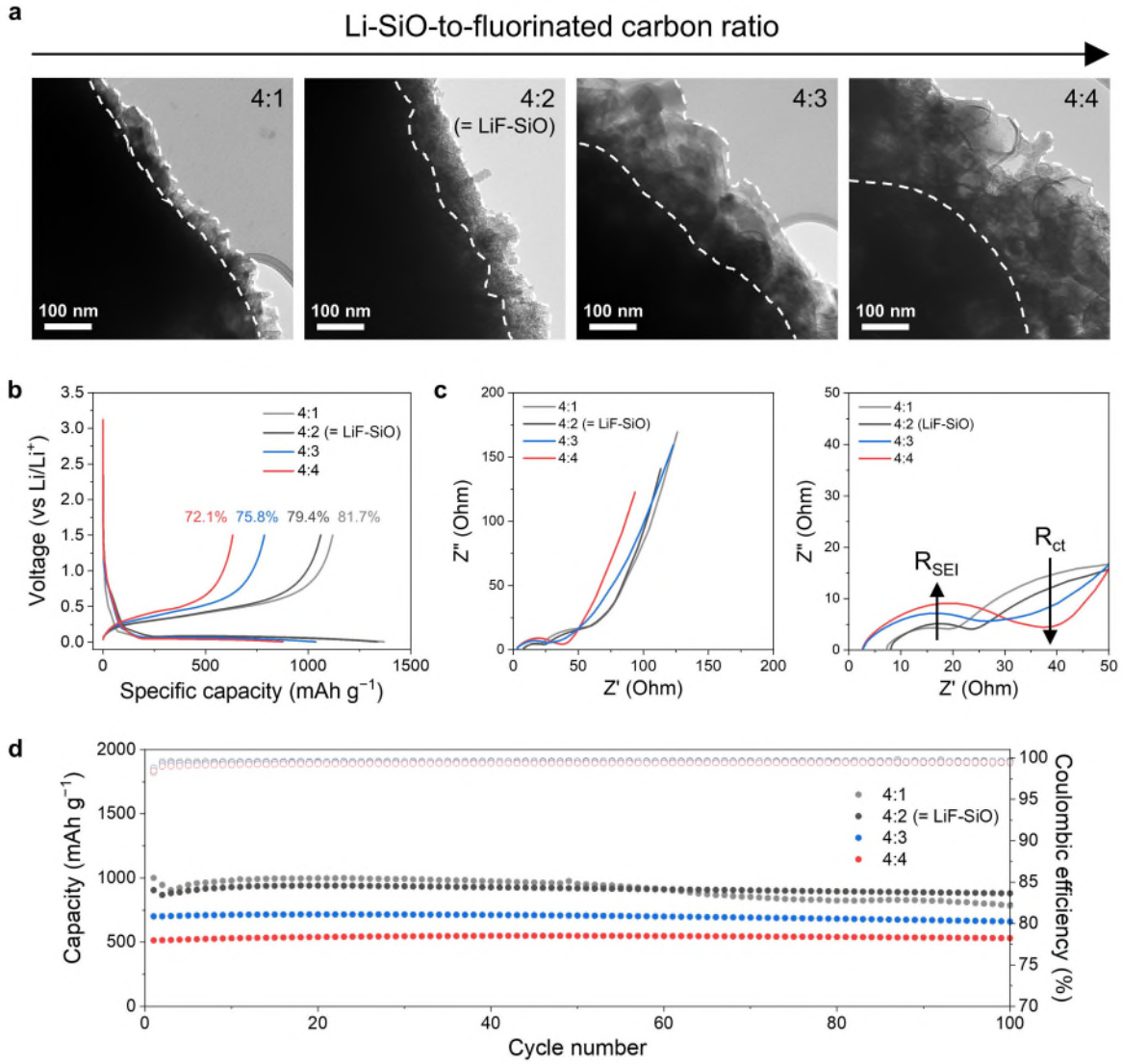

Supplementary Fig. 14 | Effects of sheath thickness on mechanical and electrochemical properties. a TEM images at varying Li-SiO-to-fluorinated carbon ratios, **b** corresponding galvanostatic charge/discharge profiles, **c** Nyquist plots after the formation cycle, and **d** cycle stability at 0.5 C.

[10 page] *"However, the a-LiF/F-doped carbon sheath, as demonstrated by selected area electron diffraction (SAED) pattern and EELS spectrum, is capable of delivering effective charge transport without kinetic penalties, while providing sufficient coverage for mechanical resilience against volumetric changes[43]. Importantly, coating layers thicker than those in LiF-SiO (>100 nm with high fluorinated carbon content) impose kinetic penalties and reduce initial Li reversibility (Supplementary Fig. 14)."*

Comment 1-8: *What criterion defines the "residual stress" Raman peak selection, and how sensitive are stresses to peak-fit choices and local texture?*

Response 1-8: We thank the reviewer for this important question regarding our residual stress determination. We used the first-order Raman band of crystalline Si at ~520 cm^{-1} as the stress probe. For each spectrum, a background was subtracted, and the extracted peak position was converted to stress using the calibrated relation $\Delta\omega = -4.4\sigma$ (σ in GPa), obtained from high-pressure Raman measurements on crystalline Si under hydrostatic loading (*Nano Energy* **2016**, 22, 105–110). This establishes a direct correspondence between peak shift and hydrostatic stress in the Si domains.

To assess the robustness of our stress determination, we performed systematic fitting with varying initial parameters and fit ranges. The resulting peak positions showed variations of less than 0.3 cm^{-1}, corresponding to stress uncertainties of approximately ± 0.07 GPa. The systematic evolution of both peak position and FWHM before/after cycling further validates the physical significance of our measurements, as stress-induced lattice distortion manifests consistently in both parameters.

Our LiF-SiO material consists of micrometer-scale particles (5 μm) containing nanoscale Si domains (3–5 nm) randomly dispersed within an amorphous SiO_2 matrix. Critically, our Raman measurements sampled multiple locations across the electrode, with multiple acquisitions at each location. Additionally, each individual measurement inherently samples multiple nanodomains within particles and many randomly oriented particles, providing two-level orientation averaging: (1) within each particle, and (2) across particles. Consequently, our Raman signal represents an ensemble average over diverse crystallographic orientations rather than single-crystal behavior. Orientation-dependent phonon shifts are therefore largely averaged out, with any residual variation appearing in peak width (FWHM) rather than as multiple competing peak positions. Within the resolution of our setup, the dominant source of peak shift is lithiation-induced stress, and our fitting protocol effectively minimizes the influence of local texture on the reported residual stress values.

Reviewer# 2

Comments: *This manuscript presents a synthetic strategy that creates crystalline lithium fluoride (c-LiF) domains in micrometer-scale SiO particles and forms a conductive outer sheath. The precise control of c-LiF domain size through the Hall-Petch relationship and the rule of mixtures effectively improves both yield strength and Young's modulus of Si-based materials. The study systematically addresses mechanical failures in Si-based anodes through theoretical design principles and detailed structural characterization, thereby enabling fast-charging and energy-dense operation. Overall, this work could be suitable for Nature Communications, provided the points below are addressed.*

Response: We sincerely thank the reviewer for their constructive feedback. We have tried our best to address the reviewer's concerns/comments through point-by-point responses, and the manuscript has been revised accordingly to enhance its quality and clarity. The revised or newly added sentences in the revised manuscript are highlighted. We hope that the manuscript is now ready for publication in *Nature Communications*.

Comment 2-1: *While the authors provide a comprehensive discussion of various degradation mechanisms, including elastic/plastic deformation and fatigue, it would be helpful to expand the explanation of fatigue phenomena, as this concept may be less familiar to some readers in the lithium-ion battery community.*

Response 2-1: We appreciate the reviewer's powerful comments that help strengthen our work. During electrochemical cycling, the repeated volumetric expansion and contraction of Si generate cyclic stresses within the particle or composite structure. The magnitude of these stresses scales with Si particle (or Si domain in composite materials) size; below ~150 nm, individual stress levels remain insufficient to cause immediate fracture (*ACS Nano* **2012**, 6, 1522–1531). However, when such sub-yield stresses are repeatedly applied over many cycles, the cumulative mechanical loading progressively weakens the material through a process called fatigue. Fatigue causes crack initiation and propagation not through a single catastrophic event, but through accumulated damage from each cycle (Fig. R5).

[Figure Redacted]

Fig. R5. Mechanical characterizations of Li metal. (A-C) In-situ tensile testing and (D-F) fatigue testing of Li metal with a maximum stress of 0.65 times its tensile strength. The scale bar is 300 μm (*Science* **2025**, 388, 311).

Since the threshold for fatigue failure increases with yield strength, elevating strength through c-LiF size engineering directly enhances fatigue resistance by expanding the safe operating window for cyclic loading. Post-mortem SEM analysis (Fig. **5**d) confirms this improvement: LiF-SiO particles maintain structural integrity after extended cycling, while bare SiO exhibits extensive cracking and pulverization—characteristic signatures of plastic deformation with fatigue failure. Therefore, our electrochemical cycling data, combined with this microstructural evidence, provide a compelling demonstration of enhanced fatigue resistance resulting from strength improvement. In response, we have added a corresponding discussion in the revised manuscript. Please see the revised manuscript.

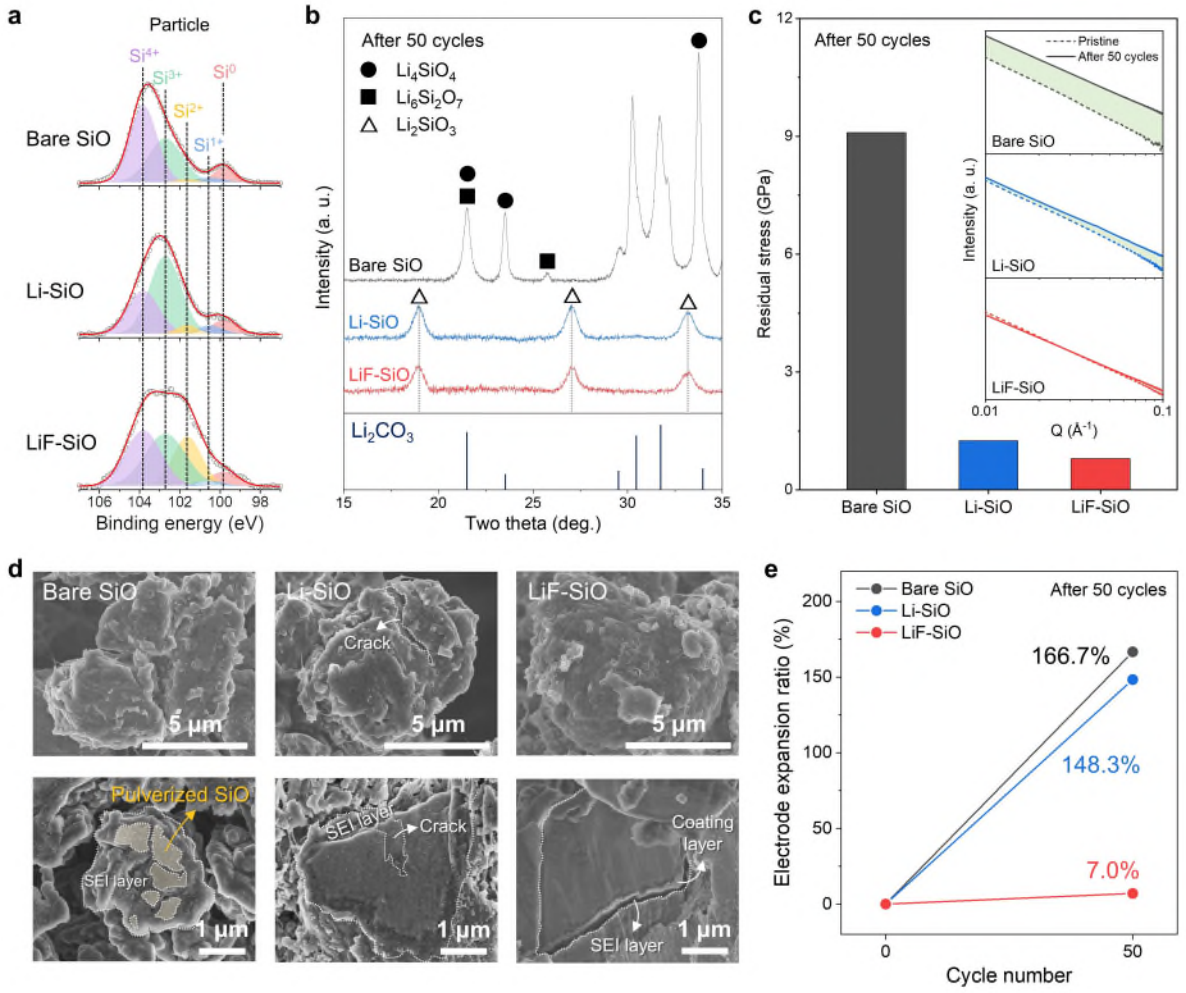

Fig. 5 | Chemo-mechanical characteristics of LiF-SiO after repeated (de)lithiation process. a Si 2p XPS spectra of bare SiO, Li-SiO, and LiF-SiO particles. **b** XRD patterns and **c** residual stress of bare SiO, Li-SiO, and LiF-SiO electrodes after 50 cycles at 2C (Inset: SAXS intensity profiles of the three electrodes). **d** Magnified SEM images (top) and cross-sectional views prepared by ion milling (bottom) of bare SiO, Li-SiO, and LiF-SiO electrodes after 50 cycles at 2C. **e** Electrode expansion ratio of bare SiO, Li-SiO, and LiF-SiO after 50 cycles at 2C.

[7 page] *"This strength–modulus synergy addresses two distinct failure modes arising from the hoop stress. First, high strength mitigates plastic deformation and potential fatigue. Notably, fatigue is defined as the process where repeated (de)lithiation cycles impose continuous mechanical loading (despite individual stress levels remaining below the yield strength) that causes material degradation and cracking, which is particularly critical in Si-based anodes. Since the threshold for fatigue failure increases with yield strength, elevating strength directly enhances fatigue resistance. Second, increased modulus minimizes mechanical strain under applied stress, thereby regulating volumetric changes and microstructural collapse."*

Comment 2-2: *The manuscript would benefit from a quantitative comparison of volume expansion behavior between bare SiO and LiF-SiO particles after lithiation. Such measurements (for example, by comparing particle sizes in SEM images of fully lithiated materials) would provide additional evidence for the claimed mechanical improvements.*

Response 2-2: We appreciate the reviewer's powerful comment regarding particle-level mechanical improvement. Following the reviewer's valuable suggestion, we performed a cross-sectional analysis of individual particles within electrodes after the first lithiation. Cross section polisher (CP) coupled with SEM enabled precise visualization of particle dimensions embedded in the electrode matrix. All cross-sectioned particles displayed in each image were analyzed to quantify the mean Feret diameter using ImageJ software (at least 50 particles per sample to ensure statistical reliability). As shown in Supplementary Fig. 22, bare SiO particles exhibit severe dimensional changes from 4.24 μm to 6.94 μm (63.7%), and the corresponding electrode thickness increases by 72.3%. Similarly, Li-SiO particles show a 53.9% increase in diameter (3.95 μm → 6.08 μm) and electrode-level expansion of 64.9%. Remarkably, mechanically reinforced LiF-SiO particles exhibit only 18.9% increase in particle size (4.34 μm → 5.16 μm), with the electrode thickness increasing 22.4%.

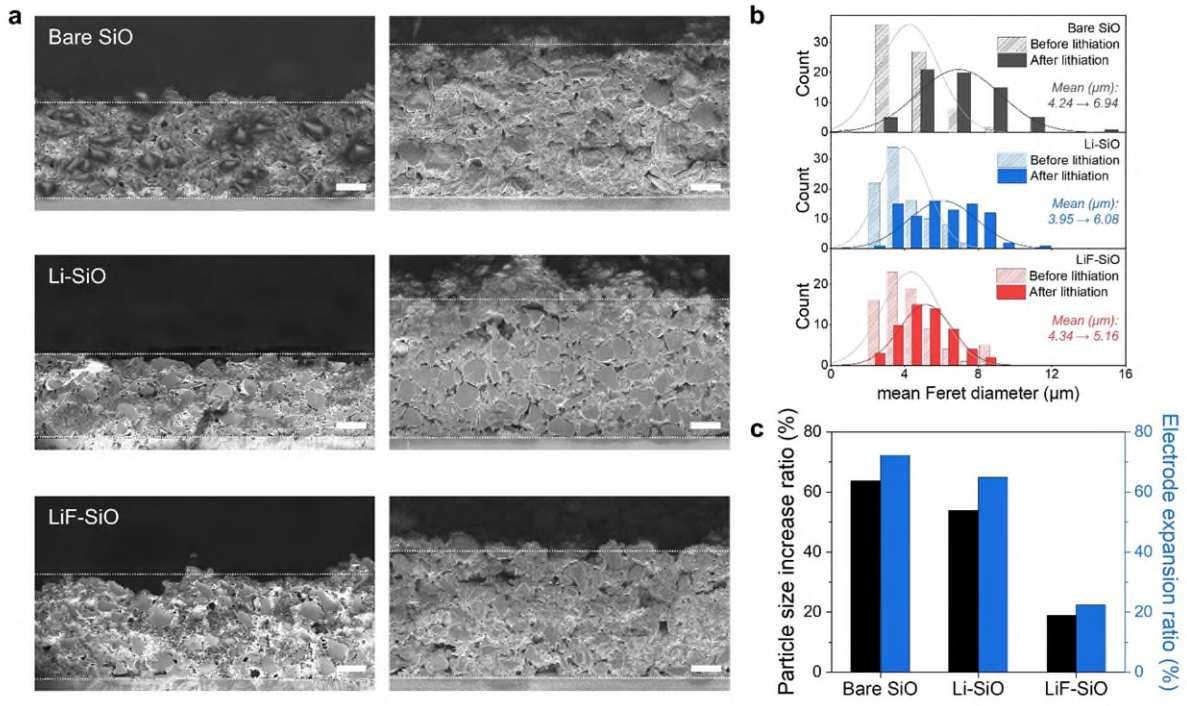

Supplementary Fig. 22 | CP–SEM analysis. a Cross-sectional SEM images of bare SiO, Li-SiO, and LiF-SiO particles within electrodes before (left) and after (right) the first lithiation, prepared using cross section polisher (CP). **b** Distribution of particle sizes (mean Feret diameter)

before and after the first lithiation, and **c** Particle size increase and electrode expansion ratios in bare SiO, Li-SiO, and LiF-SiO electrodes after the first lithiation. Scale bars, 10 μm.

To confirm that this particle-level mechanical constraint translates to electrode-level volumetric stability, we further conducted in situ thickness measurements of bare SiO, Li-SiO, and LiF-SiO electrodes during the initial 3 cycles. As shown in Supplementary Fig. 23, bare SiO and Li-SiO electrodes exhibit severe volumetric expansion of 86.0% and 73.3% during the first lithiation, respectively. After one formation cycle, their irreversible thickness increases converge to 63.2% and 49.3%, respectively, indicating persistent structural instability. In contrast, the LiF-SiO electrode exhibits significantly suppressed initial lithiation expansion, with only 19.9% expansion, and an irreversible thickness increase of merely 3.6% after the same formation cycle.

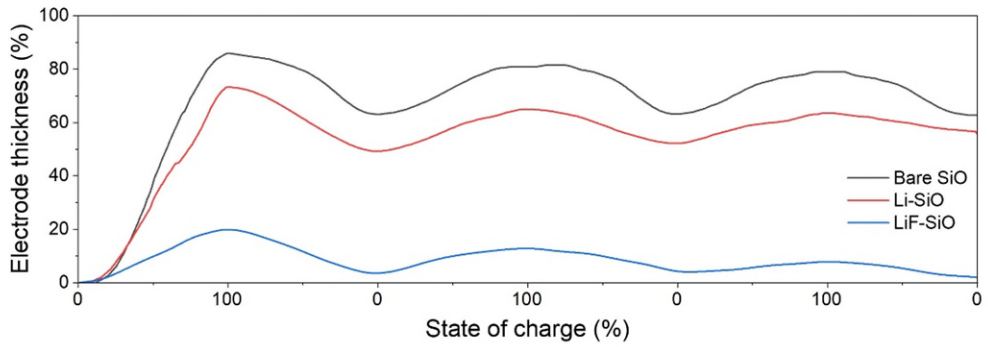

Supplementary Fig. 23 | Electrode swelling analysis. In situ thickness measurements of bare SiO, Li-SiO, and LiF-SiO electrodes during the initial 3 cycles.

This substantial difference directly reflects how particle-level mechanical reinforcement governs electrode-level volumetric stability. Elevated strength and modulus suppress plastic deformation and permanent volume changes within individual particles, which collectively prevent the accumulation of irreversible expansion throughout the electrode. These observations agree excellently with the expansion ratios observed after 50 cycles. The LiF-SiO electrode maintains a compact structure with minimal SEI thickening, as shown in post-mortem particle SEM images (Fig. **5**d), whereas bare SiO and Li-SiO electrodes suffer from severe electrode expansion and microscopic degradation. The consistent volumetric behavior captured by in situ electrode thickness measurements and CP–SEM analysis corroborates that the incorporation of optimized LiF domains effectively mitigates electrode-level swelling throughout prolonged cycling, validating our proposed Type C architecture design strategy. In this regard, we have added an expanded discussion in the revised manuscript and

Supplementary Information. Please see the revised manuscript and Supplementary Figs. 22 and 23.

[14 page] *"These particle-scale advancements translated to macroscopic electrode integrity. The optimized c-LiF incorporation in LiF-SiO not only suppressed phase separation but also imparted particle-level mechanical reinforcement, collectively reducing stress susceptibility and volumetric fluctuation. Cross-sectional polisher (CP) coupled with SEM revealed that LiF-SiO particles exhibited only 18.9% increase in particle size (mean Feret diameter) after the first lithiation, substantially lower than bare SiO (63.7%) and Li-SiO (53.9%) (Supplementary Fig. 22). In situ electrode thickness measurements demonstrated that this particle-level mechanical constraint directly manifested in electrode-level stability. During the first lithiation, LiF-SiO electrodes expanded only 19.9% compared to 86.0% (bare SiO) and 73.3% (Li-SiO), with irreversible expansion after the formation cycle reaching 3.6% versus 63.2% (bare SiO) and 49.3% (Li-SiO) (Supplementary Fig. 23). Expansion ratios after 50 cycles at 2C further quantified this sustained advantage; 166.7% (bare SiO), 148.3% (Li-SiO), and 7.0% (LiF-SiO) (Fig. 5e and Supplementary Fig. 24). Similarly, EIS measurements confirmed that LiF-SiO electrode substantially reduced internal impedance, …"*

[21 page] *"… revealed the SEI thickness and the extent of particle cracking and pulverization after cycling. Cross section polisher (CP, IB-19520CCP, JEOL) coupled with SEM (GeminiSEM 560, ZEISS) was utilized to visualize particle-level and electrode-level changes after the first lithiation. All cross-sectioned particles displayed in each image were analyzed to quantify the mean Feret diameter using ImageJ software (at least 50 particles per sample to ensure statistical reliability). In situ measurement of electrode thickness evolution during the initial 3 cycles was conducted using an HS Swell Analysis Cell (Wellcos) with $Li(Ni_{0.80}Co_{0.10}Mn_{0.10})O_2$ (NCM811) cathode as the counter electrode at an N/P ratio of ~1.05 to attribute the measured thickness changes predominantly to the anode. The physical and chemical characterization of both the particle interior and its outermost region …"*

Comment 2-3: *While Fig. 4f presents the influence of the a-LiF/F-doped carbon layer on SEI formation in the LiF-SiO electrode, further characterization using XPS depth-profiling would strengthen the proposed mechanism and enhance understanding of the compositional changes at the interface after cycling. The composition and structure of the interphase layer significantly influence the fast-charging performance of Si-based anodes (ref, Nature Communications, 2025, 16, 7956). A related discussion would help strengthen the understanding of the as-fabricated Si-based anode materials.*

Response 2-3: We thank the reviewer for this valuable suggestion. In response, we conducted XPS depth profiling on the LiF-SiO electrode after the formation cycle to elucidate the depth-

resolved compositional evolution of the interfacial layer (Supplementary Fig. 18). The analysis revealed a thin SEI with limited accumulation of resistive electrolyte decomposition products throughout the interface, contrasting with the thick organic-rich SEI layers typically observed in conventional Si-based anodes. Importantly, the pre-existing a-LiF/F-doped carbon layer persists beneath the SEI, maintaining its dual functionality of ionic (a-LiF) and electronic (F-doped carbon) conduction and thereby enabling fast-charging performance. Consistent with the suggested reference (*Nature Communications* **2025**, 16, 7956), we emphasize that the interphase composition critically determines the fast-charging capability in Si-based anodes. As the reviewer suggested, we carefully added this discussion and Supplementary Fig. 18 together with a powerful reference in our manuscript. Please see the revised manuscript.

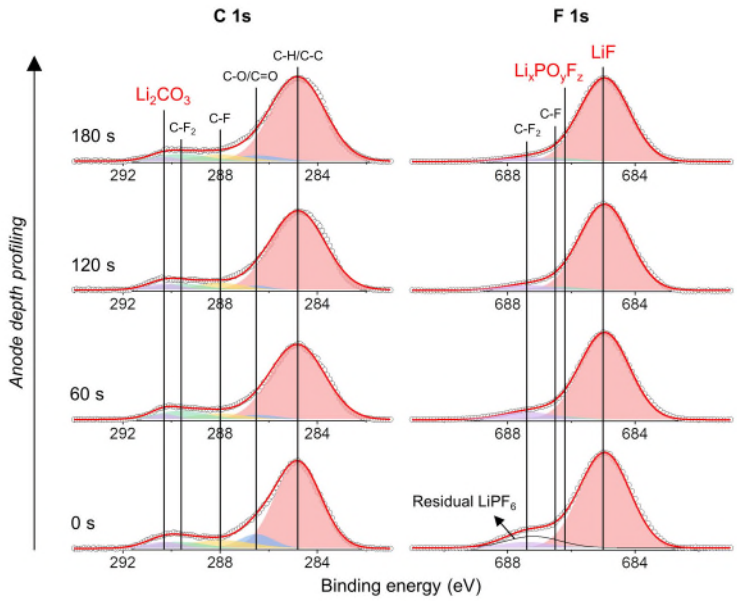

Supplementary Fig. 18 | XPS depth profiling analysis. a C 1s and F 1s XPS depth profiling spectra of LiF-SiO after the formation cycle.

[11 page] *"In contrast, the passivating a-LiF/F-doped carbon layer in LiF-SiO suppresses electrolyte reduction, forming a thin SEI thereupon and thus creating an inorganic-rich interface with decreased impedance. XPS depth profiling further revealed limited accumulation of resistive electrolyte decomposition products throughout the interface (Supplementary Fig. 18). These minimal byproducts, together with the complementary conductive contributions of a-LiF (ionic) and F-doped carbon (electronic), collectively enable superior fast-charging performance[48]."*

[21 page] *"… X-ray photoelectron spectroscopy (XPS, K-alpha, Thermo Fisher Scientific) and solid-state Fourier transform nuclear magnetic resonance (600 MHz FT-NMR, VNMRS 600,*

Varian). Furthermore, XPS depth profiling (NEXSA, Thermo Fisher Scientific) was performed at an etching rate of 20 nm min^{-1} without air exposure. Atomic force microscopy (AFM, NX10, Park Systems) with a cantilever …"

[27 page]

*48. Ou, Y. et al. A salt-free medium facilitating electrode prelithiation towards fast-charging and high-energy lithium-ion batteries. Nat. Commun. **16**, 7956 (2025).*

Comment 2-4: *For the Young's modulus measurements reported in Fig. 2c, please specify the number of samples tested and whether the reported values represent average results with appropriate statistical analysis.*

Response 2-4: We thank the reviewer for this important comment. The Young's modulus measurements in Fig. **2**c were obtained from five independent samples (n = 5) for each material, with the reported values representing the mean. This statistical information has been added to the Methods section in the revised manuscript. Please see the Methods section in the revised manuscript.

[21 page] *"… Atomic force microscopy (AFM, NX10, Park Systems) with a cantilever (NM-RC-SEM, $k \approx 350$ N m^{-1}, $f \approx 750$ kHz) was applied to measure Young's modulus, assuming a Poisson's ratio of 0.17. Reported values represent the mean of five independent measurements (n = 5) per sample."*

Comment 2-5: *The 3D mapping data in Fig. 3c requires scale specification in the data boxes to enable better interpretation of the LiF spatial distribution observed in the TOF-SIMS analysis.*

Response 2-5: We appreciate that the reviewer pointed out a missing point. All TOF-SIMS analysis in this manuscript was performed on a 250 μm × 250 μm area. We have carefully added to the Methods section in the revised manuscript. Please see the Methods section in the revised manuscript.

[21 page] *"… Time-of-flight secondary ion mass spectrometry (TOF-SIMS, TOF-SIMS 5, ION TOF) was exploited to study the in-depth chemical bonding distribution (250 μm × 250 μm area), deploying Bi^+ (25 keV, 1.00 pA) as a primary beam and Cs^+ (2 keV, 150 nA) as a sputter beam under vacuum (< 5.0 × 10^{-10} Torr)."*

Reviewer# 3

Comments: *The authors proposed a method for stabilizing the electrochemical activity of silicon-based electrodes - a problem which has been a subject of intense investigations over the past decade. The authors demonstrated a functional full cell even in a pouch cell format.*

Despite interesting results, there is a number of experimental issues to be addressed:

Response: We sincerely thank the reviewer for their constructive feedback. We have tried our best to address the reviewer's concerns/comments through point-by-point responses, and the manuscript has been revised accordingly to enhance its quality and clarity. The revised or newly added sentences in the revised manuscript are highlighted. We hope that the manuscript is now ready for publication in *Nature Communications*.

Comment 3-1: *The article claims the formation of LiF-SiO as a general principle, however, it's formation can only be achieved if the starting material originates from LG Energy Solutions, which is not a common chemical vendor. Therefore, this raises a question about reproducibility of the presented work as the starting materials are not obvious and were not fully characterized. Thus, while this approach is industrially interesting and relevant, I am not sure if this is of a broad interest of a scientific community.*

Response 3-1: We appreciate the reviewer's concern regarding reproducibility. We would like to clarify that Li doping in SiO_x is a widely researched and industrially adopted strategy to overcome the low ICE of bare SiO_x (*Nano Energy* **2021**, 89, 106378; *J. Electroanal. Chem.* **2024**, 959, 118141), as shown in Fig. R6. Most commercial SiO_x materials currently incorporate Li (or Mg) doping through various synthesis methods.

[Figure Redacted]

Fig. R6. (a) Schematic illustration for the fabrication process of the d-SiO/C/LSO (*J. Electroanal. Chem.* **2024**, 959, 118141).

While specific details of the Li-doped SiO (Li-SiO) provided by LG Energy Solutions cannot be fully disclosed due to confidentiality agreements, we have added a comprehensive synthesis protocol in the Supplementary Information to ensure reproducibility. This protocol

describes the general Li doping procedure applicable to commercial SiO materials, including the material used in this study. To further address reproducibility concerns, comprehensive characterization of both the bare SiO (SEM image and particle size distribution) and the resulting Li-SiO (Li and carbon content by ICP-AES and elemental analysis; phase and structure by XRD, XPS, TOF-SIMS, and FIB–TEM) has been reported throughout the manuscript to ensure batch-to-batch consistency (Fig. R7, Fig. **3**b, and Supplementary Figs. 3, 8, 9, 12, and 13). Additionally, Li-SiO materials are commercially available from multiple vendors, including Daejoo Electronic Materials Co., Ltd. and Shin-Etsu Chemical Co., Ltd., further demonstrating the accessibility and reproducibility of this approach. Please see the Methods section in the revised manuscript.

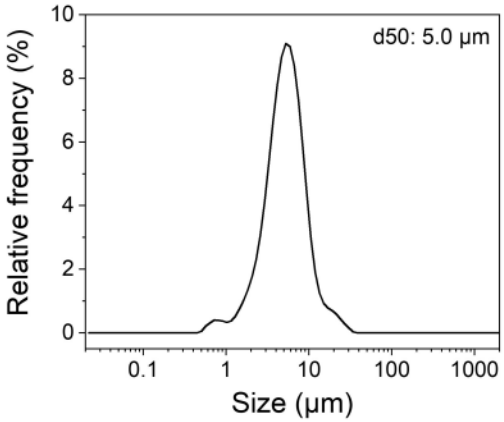

Fig. R7. Statistical particle size distribution of bare SiO (d50 = 5.0 μm).

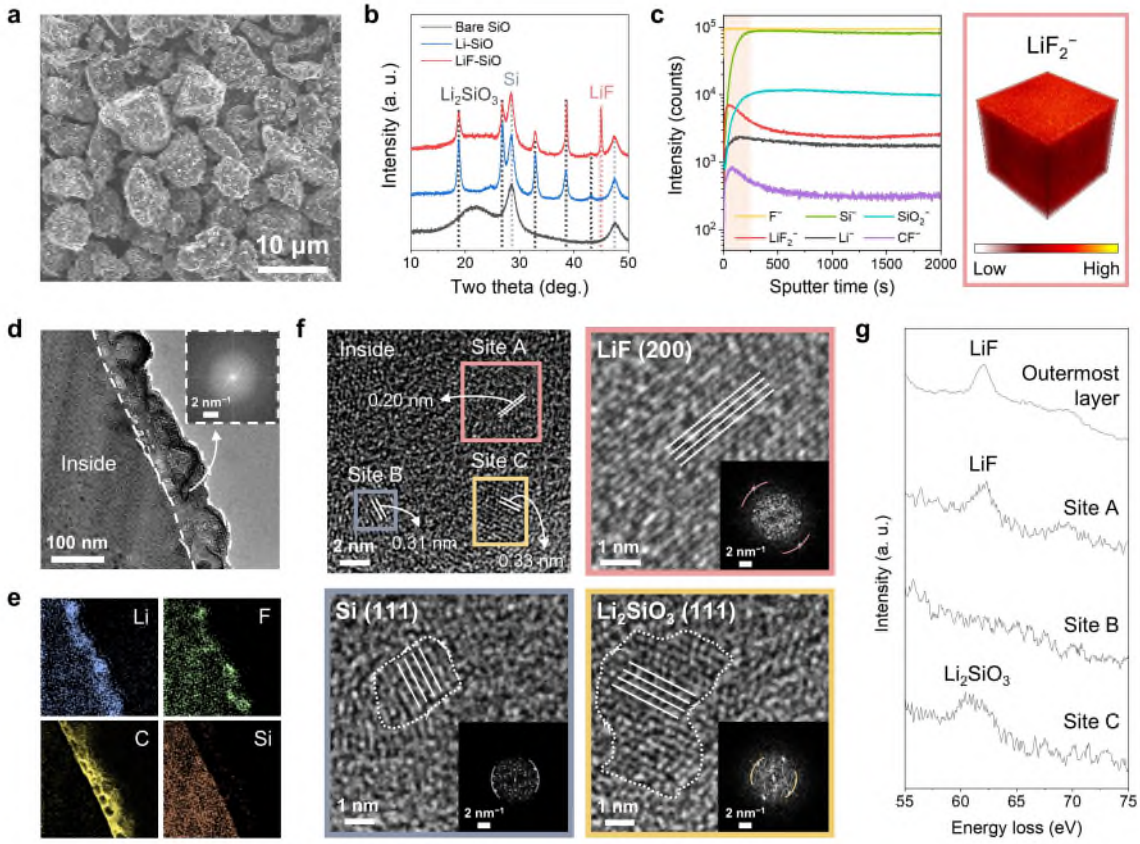

Fig. 3 | Structural characterization of LiF-SiO. a SEM image of LiF-SiO particles. **b** XRD patterns of bare SiO, Li-SiO, and LiF-SiO. **c** TOF-SIMS depth profiling results of LiF-SiO (orange region: coating layer) and corresponding 3D mapping of LiF_2^-. **d** FIB–TEM image (Inset: SAED pattern of the outermost layer) and **e** the corresponding EELS mapping of LiF-SiO. **f** Magnified FIB–TEM images of the core region within LiF-SiO (Inset: SAED patterns of each site), and **g** the corresponding EELS spectrum for each site.

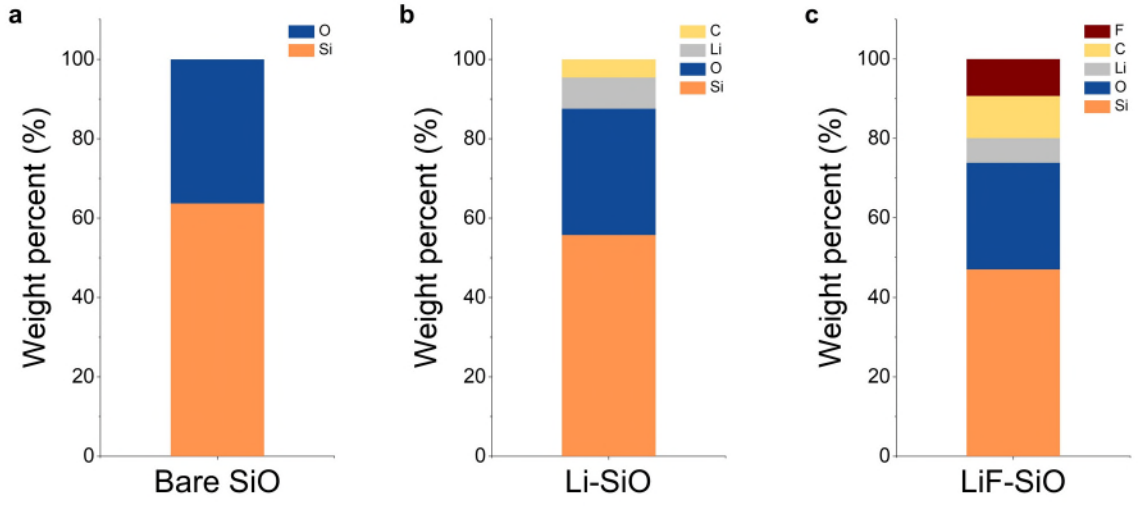

Supplementary Fig. 3 | Compositional elemental quantification. Elemental characterization of **a** bare SiO, **b** Li-SiO, and **c** LiF-SiO through ICP-AES, EA, and CIC analysis.

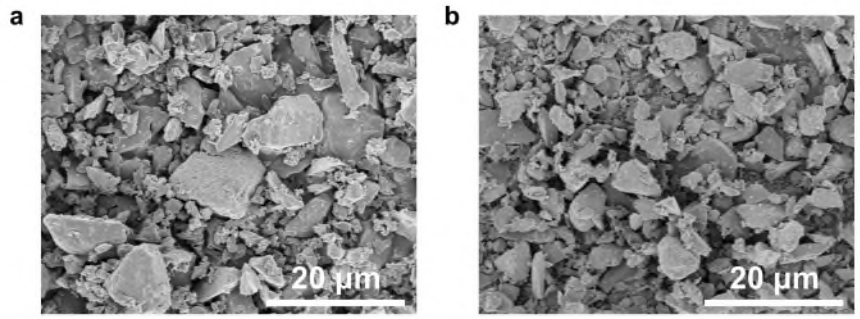

Supplementary Fig. 8 | Top-view SEM analysis. SEM images of **a** bare SiO and **b** Li-SiO particles.

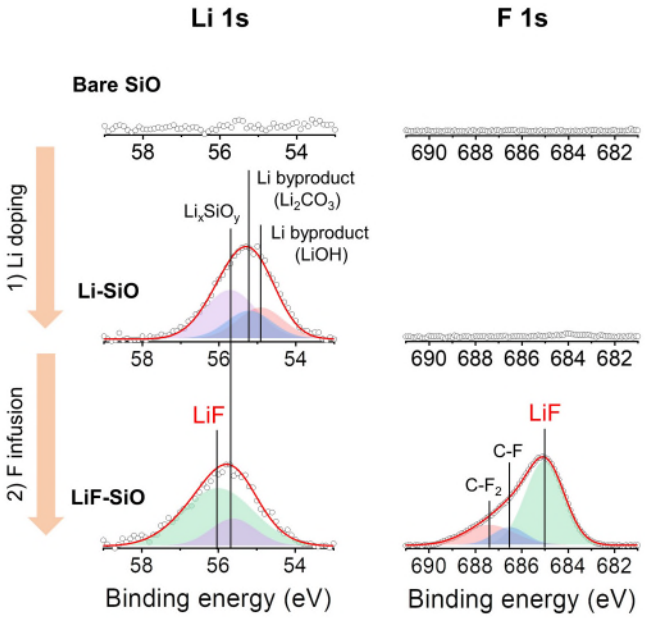

Supplementary Fig. 9 | XPS analysis. Li 1s and F 1s XPS spectra of bare SiO, Li-SiO, and LiF-SiO.

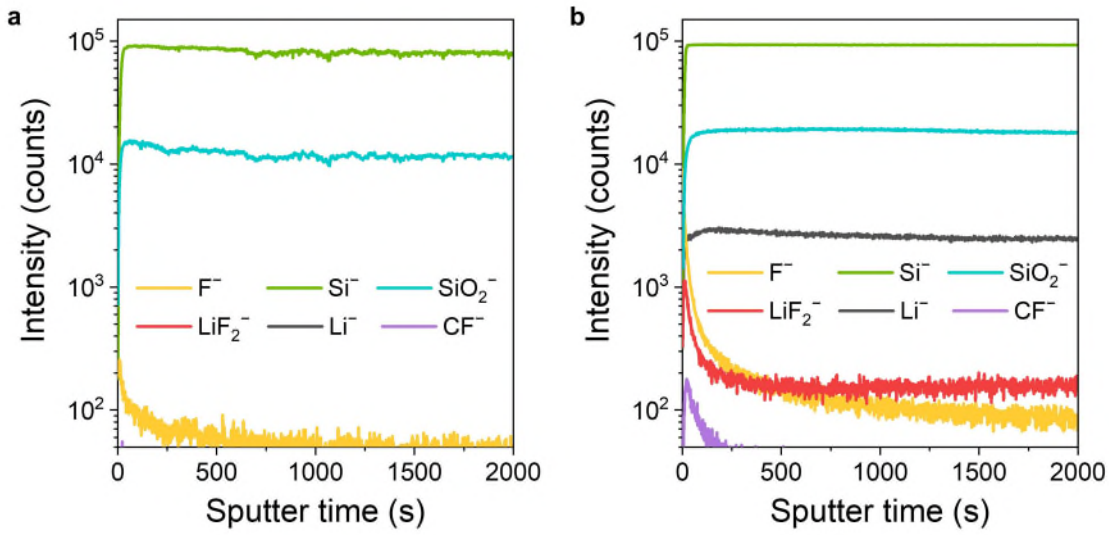

Supplementary Fig. 12 | TOF-SIMS analysis. TOF-SIMS depth profiling results of **a** bare SiO and **b** Li-SiO.

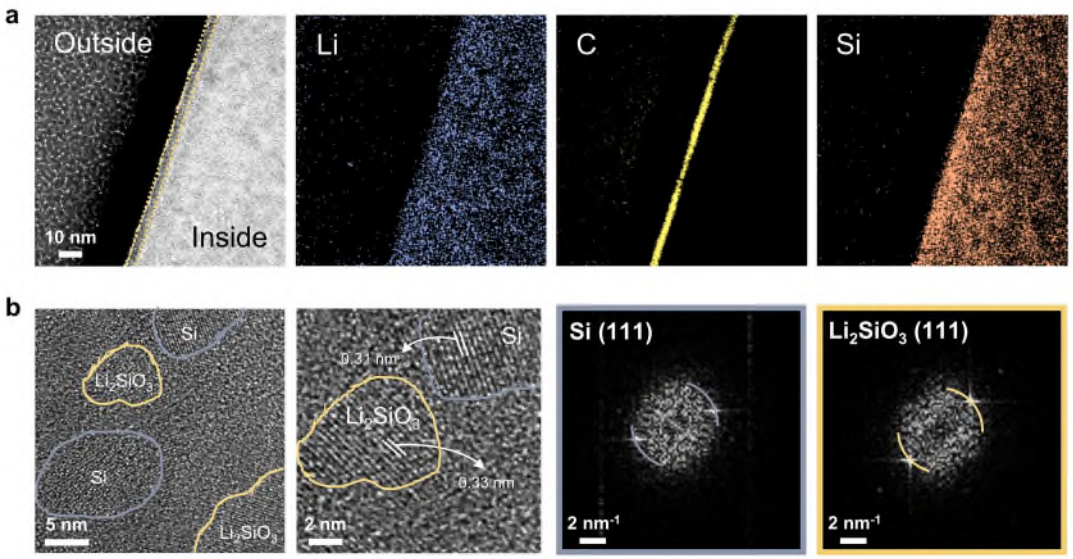

Supplementary Fig. 13 | TEM analysis. a FIB-TEM image and corresponding EELS mapping of Li-SiO. **b** Magnified FIB-TEM images of the core region within Li-SiO, with corresponding SAED patterns of each site.

[20 page] ***Synthesis of Li-SiO***

"SiO was placed in a tube furnace and heated under an argon (Ar) atmosphere. Acetylene (C_2H_2) gas was introduced to create a carbon coating on the SiO surface. After cooling to room

temperature, the recovered particles and Li compounds (typically LiH) were mixed in an Ar-filled glove box at a Li/Si ratio of 0.67. The mixed material was then heated under an Ar atmosphere to facilitate Li doping into the carbon-coated SiO. Note that specific synthetic conditions (including temperature profiles and heating durations) may vary depending on the starting SiO material and desired characteristics."

Comment 3-2: *The experimental part lack details: a) preparation - define ultrasonication, amount of toluene added to the mixture. b) Electrode preparation: why 10 % of the binder has been used? This should be justified, especially considering claimed stability. Was the electrode prepared through a dry processing or water-based (details are missing)? c) how many cells were evaluated? the presented data reflects a measurement of a single cell or average? d) Why FEC has been used in the electrolyte? Can the authors provide a comparison of electrolytes with and without FEC? e) The selected voltage window should be justified/explained. Generally, Si-based anodes are not cycled to 5 mV due to the formation of crystalline phase of lithiated silicon, which is believed to be detrimental for long-term cyclability of Si.*

Response 3-2: We appreciate the reviewer's constructive feedback, which has substantially improved the clarity and rigor of our experimental methodology. We address each point below:

a) Materials preparation:

PVDF was dissolved in DMF using an ultrasonic bath for 1 h to ensure complete mixing. Subsequently, Li-SiO was added to the solution. A total of 500 mL of toluene was then introduced as a nonsolvent to induce precipitation of fluorinated carbon onto the Li-SiO surface. These details have been added to the Methods section in the revised manuscript.

[20 page] *"PVDF (0.5 g) was dissolved in DMF (49.5 g) using an ultrasonic bath for 1 h to ensure complete mixing. Subsequently, Li-SiO (1 g) was added and stirred to achieve homogeneous dispersion. A total of 500 mL of toluene was then introduced dropwise as a nonsolvent to induce precipitation of fluorinated carbon onto the Li-SiO surface, and the resulting suspension was centrifuged three times at 3500 rpm for 10 min each. The recovered particles were dried under vacuum at 70 °C overnight, followed by a fluorine-infusion process in a tube furnace at 600 °C for 1 h under an Ar atmosphere."*

b) Electrode preparation:

Si-based materials typically require higher binder contents (≥20 wt%) to accommodate the substantial volume fluctuation during cycling. However, to emphasize the practical viability of our material, we deliberately reduced the binder content to 10 wt%, demonstrating that our mechanically reinforced structure can maintain structural integrity even under this lean-binder

condition. The electrode slurry was prepared using N-methyl-2-pyrrolidone (NMP) as the solvent, following standard wet-processing protocols. This information has been added to the Methods section in the revised manuscript.

[22 page] *"Anode slurries were prepared by blending active materials, poly(acrylic acid) (PAA) binder, Super P, and single-wall carbon nanotube (SWCNT) in a mass ratio of 80:10:9:1 (reduced binder content for practical application). The resulting N-methyl-2-pyrrolidone (NMP)-based homogeneous slurry was then cast onto Cu foil … The electrodes were dried in a vacuum oven at 120 °C overnight."*

c) Cell evaluation statistics:

At least four independent cells were fabricated and evaluated per condition to ensure reproducibility. The presented electrochemical data represent cells exhibiting average properties among the tested samples.

[22 page] *"All electrochemical characterizations of the coin-type cells were performed using a galvanostatic battery cycler (WBCS3000, Wonatech) and potentiostat (VMP3, Biologic). At least four cells per condition were tested, and the displayed data represent average properties. Half cells were tested within potential windows of 0.005–1.5 V for one formation cycle ..."*

d) FEC additive rationale:

Fluoroethylene carbonate (FEC) was incorporated as an electrolyte additive based on its well-established benefits for Si-based anodes and its widespread adoption in commercial cells. FEC undergoes preferential reductive decomposition (LUMO energy: 0.98 eV) compared to ethylene carbonate (EC, 1.17 eV), forming a stable LiF-rich SEI that exhibits superior chemical stability and mechanical robustness—critical attributes for accommodating the drastic volume changes of Si (*J. Power Sources* **2006**, 161, 1254–1259). The LiF and Si–F components in the SEI possess high binding energies (Si–F: 565 kJ/mol), effectively suppressing continuous electrolyte decomposition and parasitic reactions during repeated cycling. Given that FEC is a standard component in practical Si-anode formulations, we focused our evaluation on this industrially relevant electrolyte composition. In this regard, we have added this discussion in the Methods section in the revised manuscript.

[22 page] *"Coin-type cells (CR2032, Wellcos) were assembled in an Ar-filled glove box employing polypropylene (PP) membranes (Celgard 2400) as separators, Li metal as*

counter/reference electrodes, and 1.3 M $LiPF_6$ in ethylene carbonate (EC)/diethyl carbonate (DEC) (3:7, v:v) with 10 wt% fluoroethylene carbonate (FEC) as the electrolyte. FEC was incorporated as a standard electrolyte additive for Si-based anodes to form a LiF-rich solid-electrolyte-interphase (SEI) that accommodates their large volume changes. All electrochemical characterizations of the coin-type cells were performed using a galvanostatic battery cycler (WBCS3000, Wonatech) and potentiostat (VMP3, Biologic).”

e) Voltage window selection:

We acknowledge the reviewer's insightful comment regarding the crystalline $Li_{15}Si_4$ phase formation at deep lithiation. In our protocol, the initial one formation cycle was conducted between 0.005 and 1.5 V vs. Li/Li^+ to ensure complete activation of the Si-based material. However, all subsequent cycling was performed within a narrower window of 0.01–1.2 V vs. Li/Li^+, deliberately avoiding the potential window where crystalline $Li_{15}Si_4$ forms. This strategy prevents the detrimental phase transition while maintaining high-capacity utilization. This protocol has been clarified in the Methods section in the revised manuscript.

[22 page] *“At least four cells per condition were tested, and the displayed data represent average properties. Half cells were tested within potential windows of 0.005–1.5 V for one formation cycle to activate the Si-based material, then 0.01–1.2 V for subsequent cycles to avoid deep lithiation detrimental to cycling stability. Electrochemical impedance spectroscopy (EIS) was conducted with a frequency range of 10^6–10^{-1} Hz and a voltage amplitude of 100 mV.”*

Comment 3-3: *Figure 3. XRD peaks should be properly identified. In addtiion, a picture representing LiF2- is not clear - what is suppose to show?*

Response 3-3: We thank the reviewer for this comment that strengthens our work. In response, we have systematically identified all diffraction peaks in Fig. **3**b, assigning each feature to its corresponding crystalline phase: c-Li_2SiO_3, Si, and c-LiF. This comprehensive phase assignment has been extended to the newly added Supplementary Fig. 11, where temperature-dependent patterns including parasitic phases (crystalline SiO_2 and Li_2Si_2O5) are fully identified. These annotations provide unambiguous structural information, enabling clear tracking of phase evolution throughout the synthesis process. Please see the revised Fig. **3**b and Supplementary Fig. 11.

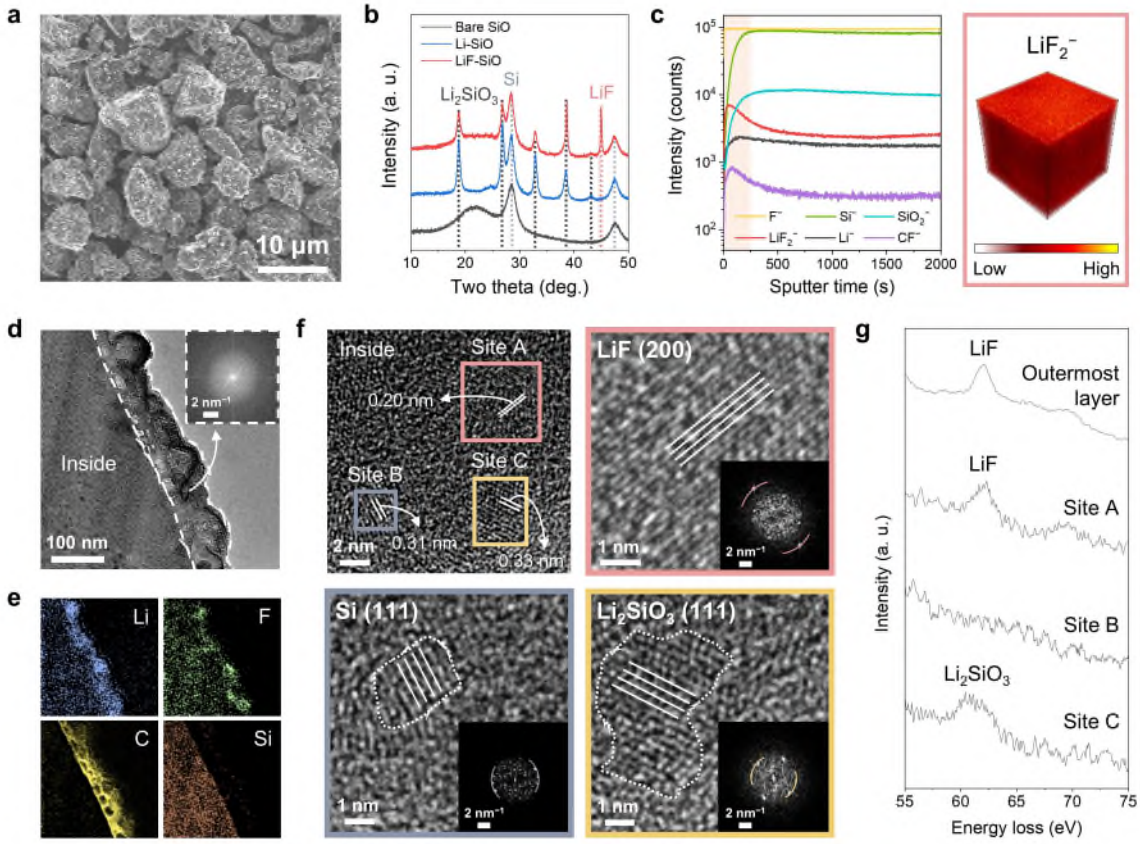

Fig. 3 | Structural characterization of LiF-SiO. a SEM image of LiF-SiO particles. **b** XRD patterns of bare SiO, Li-SiO, and LiF-SiO. **c** TOF-SIMS depth profiling results of LiF-SiO (orange region: coating layer) and corresponding 3D mapping of LiF_2^-. **d** FIB–TEM image (Inset: SAED pattern of the outermost layer) and **e** the corresponding EELS mapping of LiF-SiO. **f** Magnified FIB–TEM images of the core region within LiF-SiO (Inset: SAED patterns of each site), and **g** the corresponding EELS spectrum for each site.

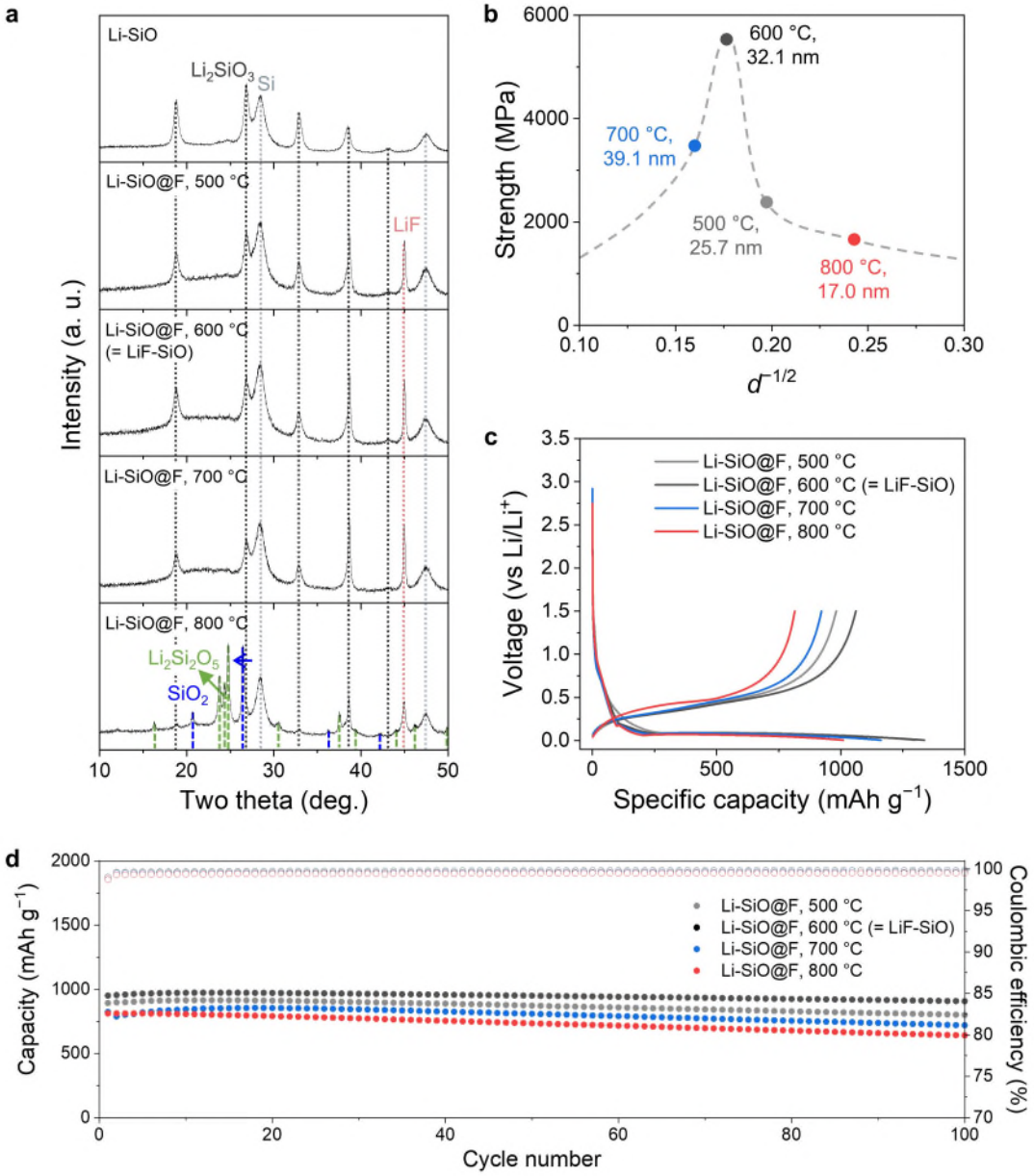

Supplementary Fig. 11 | Effects of crystalline LiF domain size on mechanical and electrochemical properties. a XRD patterns of Li-SiO(@F) before and after F infusion at varying heat treatment temperatures, **b** corresponding strength versus $d^{-1/2}$ curve, **c** galvanostatic charge/discharge profiles, and **d** cycle stability at 0.5 C.

Furthermore, regarding the LiF_2^- visualization, we clarify that this signal originates from LiF rather than representing a distinct chemical species. During TOF-SIMS analysis, the beam induces fragmentation and recombination, generating secondary ion clusters such as LiF_2^- from the underlying LiF phase. Independent characterization techniques—XPS (LiF peaks at 56.0 eV in Li 1s; 685.0 eV in F 1s spectra) and solid-state ^{19}F NMR (signals at 146.5

and 204.4 ppm)—confirmed that only LiF exists in the material. To prevent misinterpretation, we have added explicit clarification in the main text, noting that the LiF_2^- signal tracks the spatial distribution of LiF. Please see the revised manuscript.

[9 page] *"Time-of-flight secondary ion mass spectrometry (TOF-SIMS) depth profiling revealed Li (from c-Li_2SiO_3) exhibits faster outward diffusion kinetics than F inward transport due to differences in their radii and lattice diffusion mechanisms (Fig. 3c and Supplementary Fig. 12)*[41,42]*. This led to increased LiF concentration at the particle exterior, as visualized in the 3D mapping of LiF_2^-. Note that LiF_2^- detected in the TOF-SIMS originates from LiF through secondary ion cluster formation during the analysis, which tracks the spatial distribution of LiF."*

Reviewer# 4

Comments: *I co-reviewed this manuscript with one of the reviewers who provided the listed reports. This is part of the Nature Communications initiative to facilitate training in peer review and to provide appropriate recognition for Early Career Researchers who co-review manuscripts.*

Response: We sincerely thank the co-reviewer and the supervising reviewer for their constructive feedback. All comments have been carefully addressed, and the manuscript has been revised accordingly to enhance its quality and clarity.